Characterization and performance evaluation of laterite based geopolymer binder cured at different temperatures

Cyriaque Rodrigue KAZE[a,b,i,*], Patrick NINLA LEMOUGNA[c,d], Thamer ALOMAYRI[e], Hasan ASSAEDI[f], Adeyemi ADESINA[g], Shaswat Kumar Das[h], Gisèle-Laure Lecomte-Nana[i], Elie KAMSEU[b,j], Uphie CHINJE MELO[a], Cristina LEONELLI[j]

[a]Laboratory of Applied Inorganic Chemistry, Faculty of Science, University of Yaoundé I, Yaoundé, Cameroon.
[b]Laboratory of Materials, Local Materials Promotion Authority, MINRESI/MIPROMALO, Yaoundé, Cameroon.
[c]School of Chemical Engineering and Mineral Industries, University of Ngaounderé, Cameroon.
[d]Fibre and Particle Engineering Research Unit, University of Oulu, Finland.
[e]Department of Physics, Umm-Al-Qura University, Makkah, Saudi Arabia.
[f]Department of Physics, University College in AlJumum, Umm Al-Qura University, Makkah, Saudi Arabia.
[g]Department of Civil and Environmental Engineering, University of Windsor, Windsor, Canada
[h]CSIR-Institute of Minerals and Materials Technology, Bhubaneswar, Odisha, India.
[i]Institut de Recherche sur les Céramiques (IRCER, UMRCNRS 7315), ENSIL-ENSCI, Université de Limoges, CEC, 12 rue Atlantis, 87068 limoges cedex, France.
[j]Department of Engineering "Enzo Ferrari", University of Modena and Reggio Emilia, ViaP. Vicarelli 10, 41125, Modena, Italy.
[*]Corresponding author: kazerodrigue@gmail.com (Rodrigue Cyriaque Kaze)

Tel : 00237673259397/00237696963912 ; Fax: 00237222223720

Characterization and performance evaluation of laterite based geopolymer binder cured at different temperatures

Abstract

This paper presents the results of experimental evaluation of curing conditions on the microstructure and performance of geopolymer binders developed from iron-rich laterite soils. Two calcined iron-rich laterites namely LB600 and LY600 were used as solid precursors in the preparation of geopolymer binders. The geopolymer samples were cured at 20, 60 and 80°C. FTIR, XRD, EDS and DTA/TG were used to evaluate the microstructural properties of the prepared products. The performance of the binder was evaluated in terms of the compressive strengths, water absorption, porosity, bulk density and thermal conductivity. The findings from this study showed that the dissolution of the calcined laterites in 8M NaOH increased the dissolution of Al, Si and Fe elements with increasing temperature from 20 to 80 °C. This higher dissolution of the monomers further resulted to an increase in the compressive strength of the binders at 7 and 28 days. It was also found out that curing the geopolymer in the dry state resulted in higher compressive strength at all ages compared to those cured in the wet and wet-dry state. Drying shrinkage evaluation of the geopolymer samples cured between 60 and 80 °C exhibited a lower linear shrinkage due to a high degree of geopolymerization. Microstructural investigation of the geopolymer samples cured at 80 °C showed a heterogeneous compact and dense structure resulting from high polycondensation. This densified microstructure also induced an increase in the thermal conductivity from 0.65 to 0.90 W/mK and 0.75 to 0.91 W/mK for LB600 and LY600, respectively. Nonetheless, both geopolymer binders made of LB600 and LY600 laterite powders performed well in dry, wet and wet-dry conditions, and can be used for various construction applications especially in the precast industry.

Keywords: *iron-rich laterites, geopolymer, reactivity, dry-wet-dry compressive strengths, microstructure, thermal conductivity, porosity*

1. Introduction

Laterites are reddish and yellowish soils formed in tropical and subtropical areas. They are formed as a result of the alteration of kaolinite by iron minerals through the induration phenomenon. The term “Geopolymer” was coined in the 1970s by the French scientist Davidovits to classify green cementitious materials obtained from alkali activation of aluminosilicate powders at temperatures below 100 °C. The structure of geopolymers consists of repeating units of silico-oxide (Si-O-Si), silico-aluminate (Si-O-Al-O-), Ferro-silico-aluminate (-Fe-O-Si-O-Al-O-) [1–7]. Recently, the geopolymer terminology was also extended to phosphoric acid activated aluminosilicate materials [8–10].

Recent studies have shown promising results on the viability of using laterite soils as precursors for the production of geopolymers [11]. Another advantage in the use laterite soils as geopolymer precursors is their high availability in many regions of the world [12]; hence limited costs could be associated for transportation operations during the production process making laterite based geopolymers cheaper and eco-friendlier. Moreover, considering new trends and regulations on the production of clean-energy there would be an acute deficiency of fly ash in the near future, which has been one of the most commonly used solid precursor for geopolymeric binders. Hence, after the termination of thermal power plants, the laterite soils could also be an alternative to the fly ash in the production of sustainable geopolymer binders.

Laterite could be naturally available in the form of clayey form which is fine like clayed materials or indurated form which is coarser like gravel or stone. Calcined (550 °C) clayey laterite was observed to perform well in the development of geopolymers, achieving up to 45 MPa when activated with sodium hydroxide [13]. The mechanical properties of some calcined indurated laterite were also found to increase with the addition of 20 to 50 wt.% blast furnace slag to induce the formation of both C-S-H gel and N-A-S-H gel that reinforced the geopolymer

structure [14]. The effect of the silica modulus of the activating solution on the performance of geopolymer binders from iron-rich laterite calcined at 600 °C was also investigated by Kaze et al. [15]. The results from this study showed that 0.75 was the optimum silica modulus to achieve the highest compressive strength for calcined laterite. Poudeu et al. [16] combined raw laterite and calcined laterite (i.e. at temperatures of 500-600 °C) to produce a geopolymer products and found that the synthesized products can serve as a low-cost material for building houses.

Similarly, Kamseu et al. [5] combined raw iron-rich laterite with reactive silica from rice husk ash as a precursor to produce geopolymers. The findings from the study showed that new binding phases such as hinsingerite were formed. The formation of these additional products enhanced the geopolymer binder resulting in a good cohesion between different particles as well as densification of the interconnected pores in the matrix [16]. The use of meta-halloysite was also recently observed to improve the Si/Al ratio and properties of calcined iron-rich laterite based geopolymer [11]. Bewa et al. [1] successfully investigated the use of phosphoric acid as an activator in the preparation of acid activated calcined laterite.

Generally, the curing temperature is known to affect the resulting properties of geopolymers [17]. However, most of the studies on the effect of curing temperature were performed with a geopolymer made with precursors such as metakaolin, fly ash, slag and volcanic ash [4,18–28]. Hence, in order to enhance applications of laterite based geopolymers, it is important to evaluate the effect of curing temperatures on the microstructure and performance of such geopolymers. Besides, there is a high variability in terms of chemistry and mineralogy of laterites worldwide. Hence, the need to investigate the potential use of locally available laterite in the development of geopolymer composites.

This study aimed to investigate the effect of curing temperature on the performance and microstructure of geopolymer binders made from two iron-rich laterites calcined at 600 °C. The

resulting laterite-based geopolymer pastes were cured at approximately 20 °C, 60 °C and 80 °C and products characterized using Fourier transformed infrared spectroscopy (FTIR), X-ray Diffraction (XRD) and Scanning electron microscopy (SEM). Differential scanning calorimetry coupled with thermogravimetric analysis (DSC/TG) was used to study the behaviour of different phases formed under high temperatures.

The performance of the geopolymer binders was assessed in terms of the compressive strength, water absorption, porosity, apparent density, drying shrinkage and thermal conductivity. The obtained characteristics of the resulting geopolymer binders at different curing temperatures are presented and discussed in this paper. The properties of the geopolymer binders were also correlated with the microstructural properties. In order to determine the reactivity of the laterite soils investigated, the calcined iron-rich laterites were dissolved in 8M of NaOH solution. The solubility of Al, Si and Fe which are the major elements related to the formation of the amorphous phase required for geopolymerization reaction were assessed. Also, the stability of the synthesized binders in water was assessed to tailor the mechanical properties in view to study their durability in wet and wet-dry conditions for construction purposes.

2. Experimental program

2.1 Materials

The iron-rich laterites were collected from Bamenda (North-West region), this sample presented a yellow colour, and from Yaoundé (Central Region) located in Cameroon, this second sample was reddish in colour. After collection, the materials were dried, ground and sieved to obtain particles less than 60 µm. The obtained powders from both laterites were calcined at 600 °C for 4 h at a heating rate of 5 °C/min in a programmable electric furnace according to previous works [15,29]. The obtained calcined powders were labelled LB600 and LY600 for laterites obtained in Bamenda and Yaoundé, respectively.

The alkaline solution used as the activator in this study is composed of a mixture of 8M sodium hydroxide and sodium silicate. The choice of the value of NaOH was deduced from a published work investigating the effect of soda concentration on laterite geopolymerization; in particular we took the minimum, yet still efficient, value of NaOH molarity [15]. The 8M sodium hydroxide was prepared by dissolving the required amount of sodium hydroxide pellets with a purity of 99.9% in distilled water. A commercial sodium silicate solution with weight ratio SiO_2/Na_2O of 3.00 ± 0.05 was used (commercial production imported by Ingessil, Verona. Italy). The weight ratio of the sodium silicate to sodium hydroxide was fixed at 2 for all mixtures. The alkali solutions admixture was prepared at approximately 24 hours before their use to allow the solutions to cool down to room temperature.

2.2 Geopolymer binder's preparation

To prepare the geopolymer pastes, each calcined iron-rich laterites was mixed at a liquid to solid mass ratio of 0.60 based on the optimum ratio determined from previous works [15, 30]. The paste was mechanically mixed for 5 minutes in order to achieve a homogenous plastic paste. After the mixing was completed, the fresh mixture was poured into moulds of suitable geometries for the tests to be carried out. Immediately after casting, the moulds were covered with a thin film of plastic sheet to prevent water evaporation from the samples and carbonation effect on the samples.

With the aim of investigating the effect of the curing process, the geopolymer samples were divided into three series. The first series was cured at room temperature (i.e. 20 ± 3 °C) and demoulded after 24h. The second series and third series were immediately placed in an oven with a temperature of 60 °C and 80 °C, respectively for 2 hours followed by the room temperature curing until testing age (i.e. 7 and 28 days). We noticed a setting time around 43-124 min, at 20°C, as reported in a previous work [15].

Table 1 presents a detailed summary of the employed curing regime (20, 60 and 80°C) for the synthesis of the geopolymer binders from both calcined iron-rich laterites LB600 and LY600. The mixture ID in **Table 1** are based on the source of the laterite soil and curing temperature employed. For example, LB60 and LB80 indicate laterite obtained from the Bamenda region and cured for 2 hours at 60 and 80 °C, respectively.

Table 1 Labelling of the investigated geopolymeric binders

Source	Mixture ID	Initial Curing temperature (°C)
Bamenda	LB20	20 (24 h, then demoulding)
	LB60	60 (2h, then demoulding)
	LB80	80 (2h, then demoulding)
Yaoundé	LY20	20 (24 h, then demoulding)
	LY60	60 (2h, then demoulding)
	LY80	80 (2h, then demoulding)

2.3 Characterization methods

The chemical composition the raw laterites was determined using X-ray fluorescence spectrometer Bruker S8 Tiger. Before the analysis, each sample was ground to powder, mixed with lithium borated salt and then vitrified within a Pt crucible at 1060 °C. The loss on ignition at 1050 °C was considered to perform the calculation of the final chemical compositions. The mineralogical composition of the raw and calcined laterites as well as geopolymer powdered samples were identified using X-ray diffraction (XRD) with Brucker-AXS D8 Advance Debye-Sherrer type diffractometer.

Measurements were performed, using a step-scan mode in the range $5.02° \leq 2\theta \leq 80°$, with a counting time of 10.1 s per 0.02° step (2θ). Crystalline phases were identified by comparing the

peaks with PDF standards (Powder Diffraction Files) from ICCD (the International Center for Crystallography Data). In all cases, the Kα1 wavelength of copper (λ=1.5418 Å) was used.

The particle size distribution in both calcined laterites was determined using a Mastersizer 2000 Ver. 5.22 (Malvern instruments Ltd.) indicating the particle size in both materials ranged from 0.01 to 100 µm. The values of $d_{0.1}$, $d_{0.5}$ and $d_{0.9}$ were respectively 2.61, 24.10 and 65.00 µm for LB600 and 2.03, 21.02 and 62.51 µm for LY600.

Attenuated total reflectance (ATR-FTIR) Fourier transform infrared spectroscopy technique was used to determine the main characteristic chemical groups in the raw, calcined and consolidated materials. For this study, a Nicolet 6700 apparatus from Thermo Scientific was used. For the measurements, each sample was placed over a reflective crystal medium where light passed through. A portion of the light was absorbed, and the remaining energy travelled back into the instrument and then converted using Fourier transform analysis and displayed. The medium was made of a material with a high refractive index. The reaction cell was then fixed onto the diamond ATR crystal, and FTIR spectra data were recorded over the range of 4000 to 400 cm^{-1} at a resolution of 2 cm^{-1} with 32 scans.

Differential thermal and thermogravimetric analyses (DTA and TGA) were carried out between 25 °C and 1200 °C at 5 °C/min under dry air atmosphere using Labsys Evo DTA-TGA equipment from SETARAM instrumentation. The samples were previously crushed and sieved at 100 µm, then oven-dried at 40 °C for at least one week (until the achievement of no mass variation). Alumina powder, previously heated at 1500 °C for one hour, was used as reference material. Specimens and reference powders were analyzed in the platinum crucible, using aliquots of 50 mg.

Collected pieces of laterites based geopolymer series obtained from mechanical testing were used for microstructural observations using a Zeiss Ultra Plus device. The pieces were first

mounted in epoxy moulds, then polished and coated with carbon prior to the SEM examination. Analyses were performed with a backscatter electron detector, 15 kV acceleration voltage and about 8 mm working distance.

The reactivity of the calcined iron-rich laterite powders (labelled LB600 and LY600) was performed using the dissolution test methods based on past studies [31–33]. Three (3) grams of each calcined iron-rich laterite powder was poured into a polypropylene container containing 35 mL of sodium hydroxide (NaOH) 8M solution. Afterwards, the different samples contained in the beaker were preheated for 30 minutes with an electric heating plaque at the three curing temperatures of 20, 60 and 80 °C. The mixes were then stirred at 1500 rpm for 6 h at 20 °C using a centrifuge. The centrifuge was used to separate the residue and the left solution. Each sample was filtered using a 0.50 µm paper filter. Before carrying out the main elemental composition some drops of nitric acid were added to lower the filtrate pH below 2 based on the observation made by Adesanya et al. [31]. For each sample, the elemental composition in the obtained filtrate after the dissolution was analyzed using inductively coupled plasma optical emission spectroscopy (ICP-OES) equipment Optima 2000 DV (Perkin Elmer, Waltham, MA, USA). This analysis would give the percentage of dissolved Si, Al and Fe from both calcined iron-rich laterites.

2.4 Performance of geopolymer binders

The dry, wet and wet-dry compressive strengths were carried out on samples cured at 20, 60 and 80 °C after 7 and 28 days, accordingly to some previous studies [13,34,35]. The dry compressive strength indicates the samples that were cured in a dry state while the wet compressive strength indicates the samples that were immersed in water and cured in different temperatures (i.e. 20, 60 and 80 °C). The wet-dry samples indicate samples subjected to wet and dry states while subjected to various curing temperatures.

The compressive strength evaluation was carried out on cubic samples with a dimension of 50 mm using the Instron® 1195 compression machine with a displacement of 0.5 mm/min which yields a loading rate in the range of 900 to 1800 N/s in accordance with ASTM C 109 [36]. For each mixture, three samples were tested, and the average compressive strength at each age presented. The compressive strength of each sample was obtained using **Equation 1**. Where *F* and *S* represent the maximum load at failure in Newton (N) and the surface area of the samples in square millimetres (mm^2), respectively.

$$\sigma = \frac{F}{S} \qquad (\mathbf{1})$$

The apparent density, water absorption and porosity of the geopolymer binders were determined in accordance to the test methods in ASTM C 642 – 06 [37] using cylindrical samples with a height of 50 mm and height of 100 mm.

The drying shrinkage of the mixtures was evaluated using prisms samples with a dimension of 25 mm x 25 mm x 250 mm. The drying shrinkage was evaluated based on the length change following the test procedures in ASTM C 157 [38]. For each curing regime, four samples were tested and the average result presented.

3. Results and discussion

3.1 Characterization of materials

The mineralogical phases present in the raw and calcined laterites are reported in **Figure 1** and **Figure 2** for laterite obtained at Bamenda and Yaoundé, respectively. In raw laterites, the reflection peaks of goethite (α-FeO(OH) PDF# 00-046-1045), kaolinite ($Al_2Si_2O_5(OH)_4$, PDF# 01-083-4643), quartz (SiO_2, PDF# 00-046-1045); hematite (α-Fe_2O_3, PDF # 04-003-2900); ilmenite ($FeTiO_3$, PDF# 04-015-9381); maghemite (γ-Fe_2O_3, PDF# 01-084-1595) were observed, with a prevalence of goethite in LY responsible for its more reddish colour. After the

calcination of both raw iron-rich laterites at 600°C, the reflection peaks of goethite and kaolinite disappeared indicating the transformation goethite into hematite and crystalline kaolinite into amorphous metakaolinite. Thus, 600 °C appears as effective calcination temperature of iron-rich or indurated laterites for the preparation geopolymer binders.

The chemical compositions of both laterites used as aluminosilicate precursors are presented in **Table 2**. It can be seen that both materials are mainly composed of Fe_2O_3, SiO_2 and Al_2O_3 as main oxides. Besides, the sum of the main oxides in LB600 and LY600 was 84 and 82%, respectively. This chemical composition justifies their pozzolanic nature which may also make the calcined laterite suitable for potential use as supplementary cementitious materials.

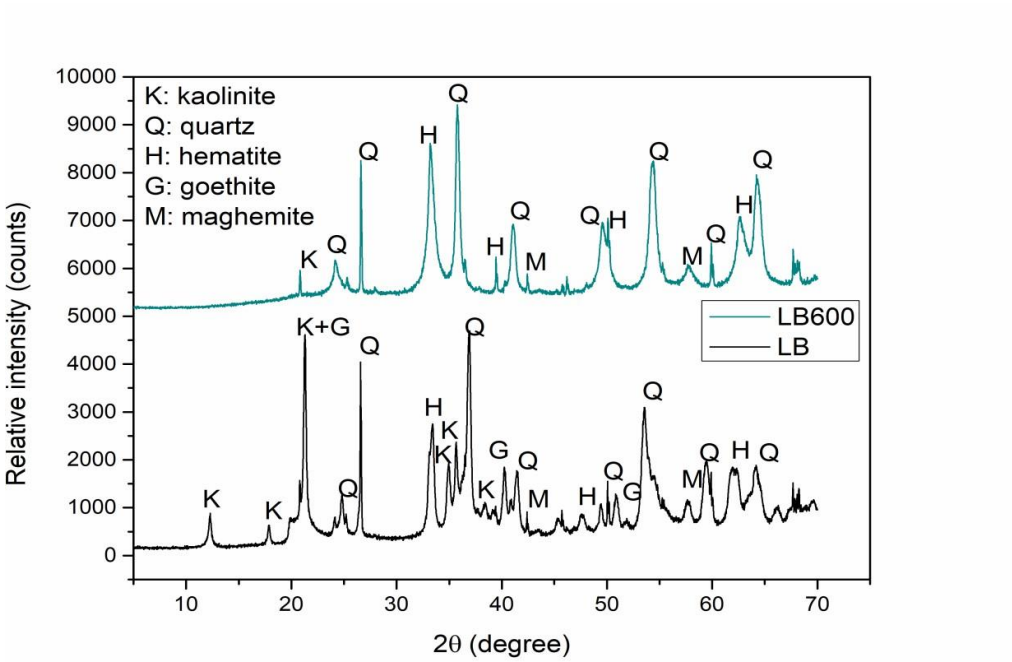

Figure 1 X-ray patterns of raw (LB) and calcined iron rich (LB600) laterites

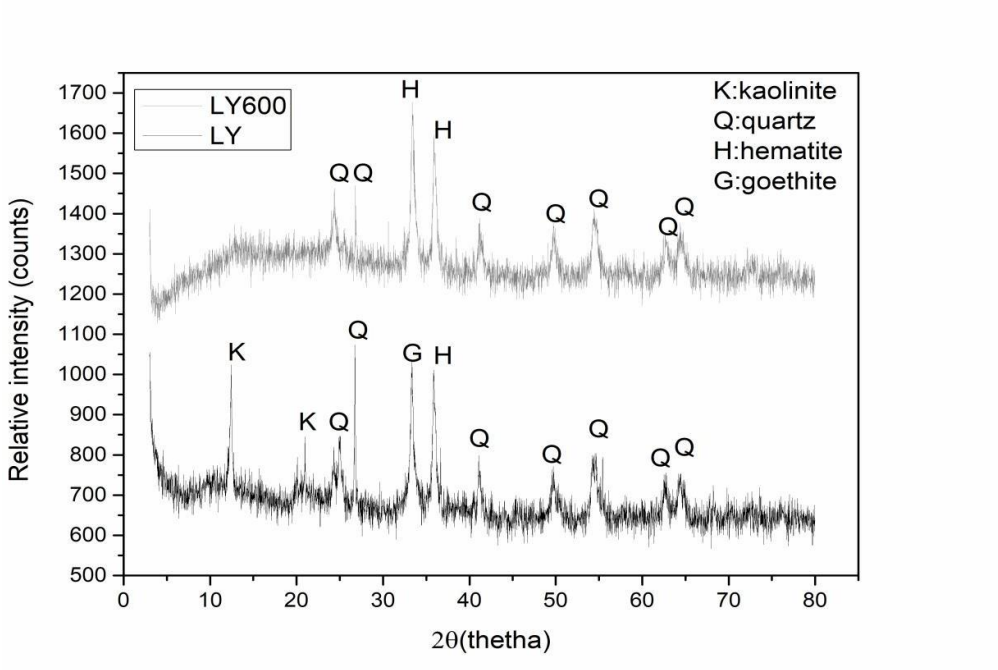

Figure 2 X-ray patterns of raw (LY) and calcined iron rich (LY600) laterites

Table 2. Chemical composition (wt%) of the two laterites (L.O.I. is loss on ignition at 1050 °C).

Oxides	LB600	LY600
Al_2O_3	17.91	14.94
SiO_2	25.56	22.30
P_2O_5	0.18	0.23
SO_3	0.05	0.03
K_2O	0.12	1.01
CaO	0.06	1.00
TiO_2	1.21	2.04
V_2O_5	0.12	0.12
Cr_2O_3	0.13	0.02
MnO	0.05	0.03
Fe_2O_3	41.01	44.30
ZrO_2	0.05	0.02
L.O.I.	13.55	13.96

Table 3. Calculated chemical composition of the two laterite-based geopolymeric binders.

Liquid to solid ratio	**0.6**	**0.6**
Oxides	**GP-LB600**	**GP-LY600**
SiO_2	21.73087	20.47609
Na_2O	9.309582	9.324686
H_2O	44.90345	44.9763
Al_2O_3	7.075789	5.911993
P_2O_5	0.071113	0.091015
SO_3	0.019754	0.011871
K_2O	0.047409	0.399673
CaO	0.023704	0.395716
TiO_2	0.47804	0.80726
V_2O_5	0.047409	0.047486
Cr_2O_3	0.05136	0.007914
MnO	0.019754	0.011871
Fe_2O_3	16.20201	17.53021
ZrO_2	0.019754	0.007914
Total	**100**	**100**

3.2 Reactivity of solid precursors

The theoretical chemical composition of the geopolymer pastes are collected in Table 3. Both geopolymeric pastes are composed mainly of Fe_2O_3, SiO_2 and Al_2O_3 while other elements (Ti, Na, K, P, Ca) exist in the trace (Table 3). Hence, we concentrated our leaching in NaOH only on these three species: Al, Si and Fe. The reactivity test results of the dissolution of both LB600

and LY600 powders in 8M of NaOH solution at different temperatures are shown in **Figure 3**. It is noticed that the dissolution in both materials was enhanced by increasing the temperature from 20 to 80 °C. Both calcined precursors recorded low solubility of Si, Al, and Fe elements at room temperature (20°C). The values were 5, 12 and 18 wt%; respectively for Si, Al and Fe from LB600, and 4, 11 and 15 wt% from LY600.

At 60 and 80 °C the solubility of Si, Al, and Fe was respectively 11, 29, 37 wt% and 14, 35 and 41 wt%, for LB600; 10, 26 and 34 wt.% and 12, 32 and 38 wt.%, for LY600. The increase in dissolved Si, Al, and Fe elements in both solid precursors suggests that the rise of curing temperature of 20 to 80 °C has favoured the dissolution of some crystalline phases (containing Al, Si and Fe elements) that released the additional Si, Al and Fe. Higher dissolution is known to favour higher reactivity during the geopolymerization process, hence, better strength development.

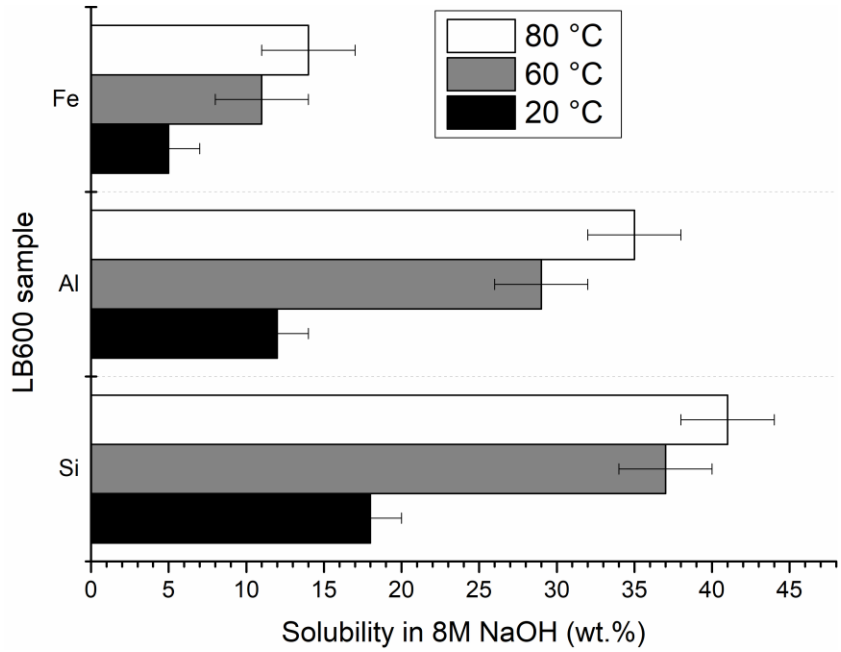

(a)

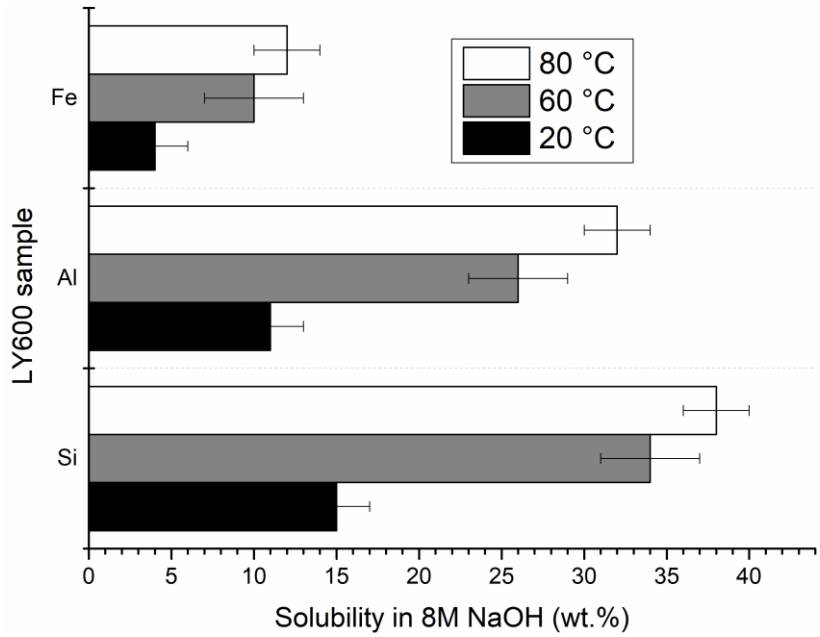

(b)

Figure 3 Dissolution rate of Al, Si and Fe at 20, 60 and 80°C **(a)** LB600 **(b)** LY600

3.3 Characterization of geopolymer products

3.3.1 Phases evolution

Figure 4 presents the infrared spectra with information related to the chemical bonds in both geopolymer products cured at 20 and 80 °C. The absorption bands located between 3391 and 3404 cm^{-1} belonging to samples cured at room temperature (20 °C), respectively in **Figure 4a** and **Figure 4b** are linked to the stretching band of O-H of water molecules. This band decreased for geopolymer products oven cured at 80 °C. This band reduction could be either due to higher consumption of water during the geopolymerization reaction or over-drying during oven curing. The second less pronounced bands at about 1640 cm^{-1} and 1652 cm^{-1} are also assigned to the bending vibration mode of the O-H bond.

In both geopolymer specimens, LB20 and LY20 (cured at 20 °C), the characteristic bands appearing between 956 and 965 cm^{-1} (belonging to geopolymer footprint). These bands shifted to higher wavenumbers 970 and 976 cm^{-1} with high intensity for both geopolymer LB80 and LY80 samples oven cured at 80 °C. This indicates that increasing the temperature from 20 to 80 °C seems to favour the high dissolution of both calcined raw materials in alkaline solution by extending the quantity of geopolymer binder within the matrix as stated by several published previous works [4,13,28]. Also, this shift could be associated with the introduction of Fe^{2+} or Fe^{3+} in -Si-O- bond as network modifier as reported by Gomes et al. [39] and Iacobescu et al. [40].

However, the less pronounced bands in both geopolymer samples at 893, 1379 and 1401 cm^{-1} are attributed to CO_3^{2-} group that formed from the reaction between unreacted sodium ions leached out of matrix with CO_2 of atmosphere namely efflorescence phenomenon. Whereas the scheduled band appearing at 880 cm^{-1} in both geopolymer products described the vibration mode of Si-O-Fe [41]. The stretching vibration mode of Si-O bond in quartz mineral [42]

detected by XRD analysis is located at 690 cm^{-1}. Finally, the last bands at 428, 537 and 562 cm^{-1} are assigned to the vibration mode of Fe-O and Si-O-Fe(Al) bonds in the geopolymer binder network, respectively [30,43].

It is worth mentioning that the absorption bands located at 893 cm^{-1} in both geopolymer series cured at 20 °C are likely linked to the C-O vibration of siderite ($FeCO_3$, Sd, JCPDS N°. 29-696) confirmed by XRD analysis. This band disappeared with increasing temperature from 20 to 80 °C suggesting the lower reactivity of iron minerals in the alkaline medium due to their precipitation as iron hydroxide in contact of the alkaline solution as reported by other authors in the literature [31,44]. The comparable observation was reported by Onisei et al. [45] during the geopolymer binders from the fayalite-rich slag.

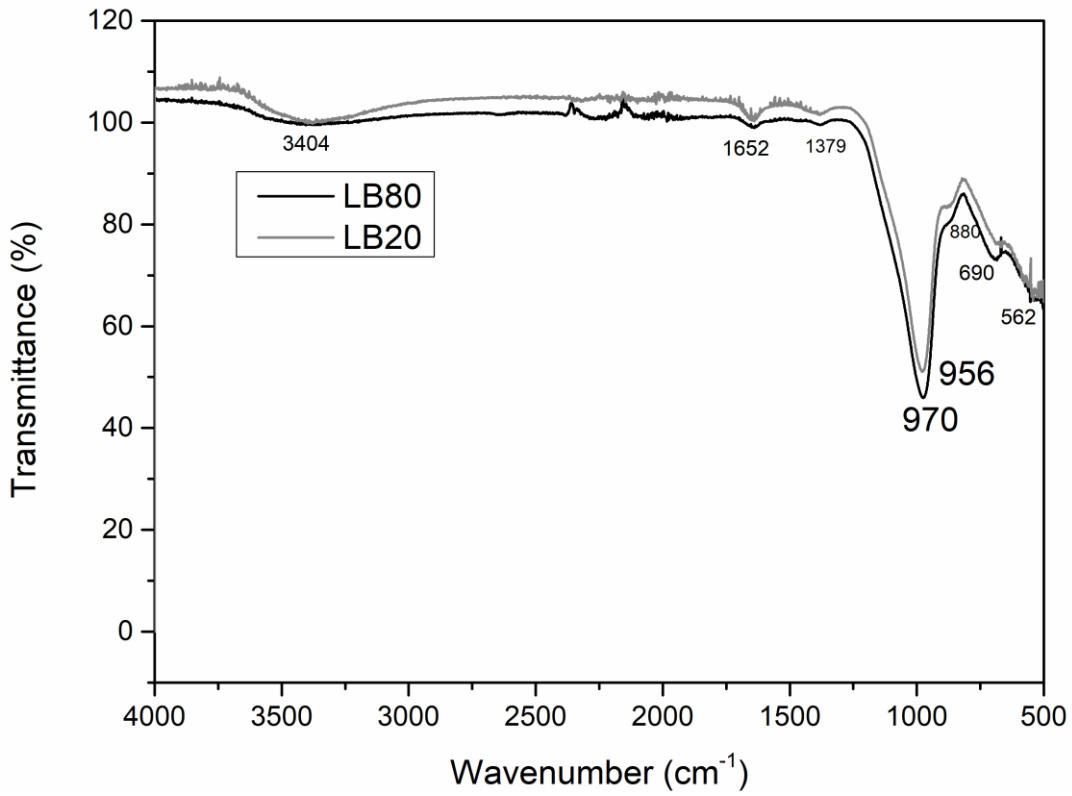

(a)

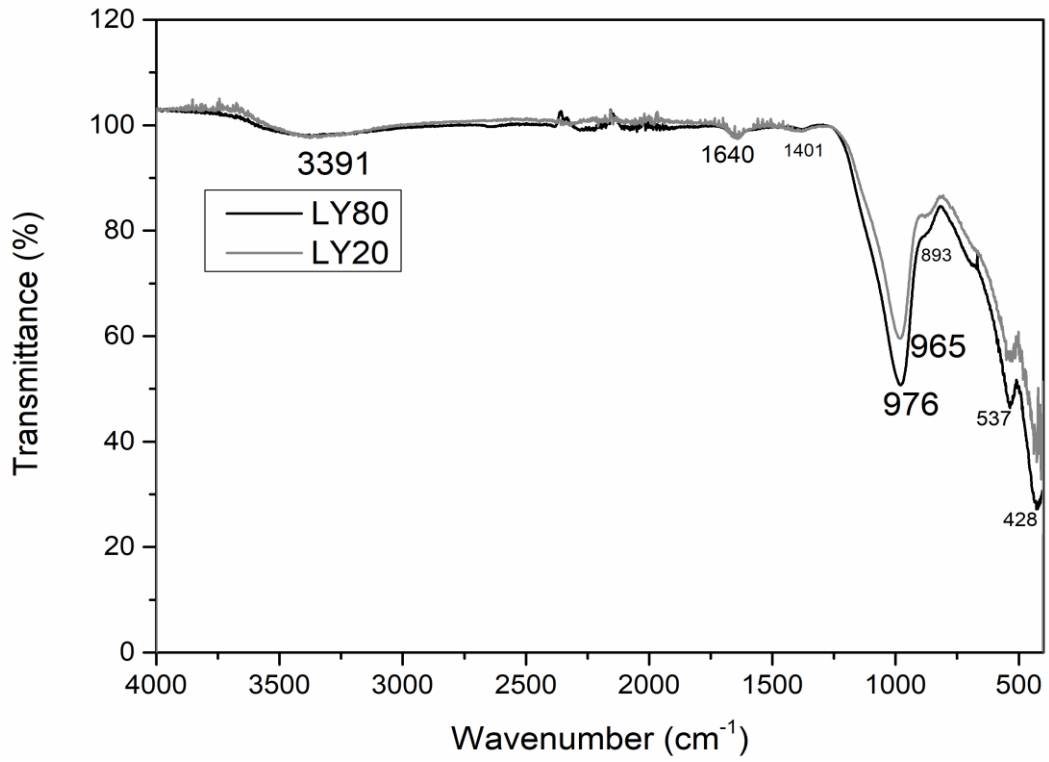

(b)

Figure 4 FTIR spectra of geopolymer composites **(a)** LB20 and LB80 **(b)** LY20 and LY80

313

Figure 5 shows the X-ray patterns of both geopolymer binder specimens obtained from LB600 and LY600 powders cured at 20 and 80 °C. Both geopolymer series appeared amorphous and exhibited a pronounced hump located between 20 and 30° 2Θ range which justifies the effective formation of geopolymer binder obtained from the dissolution of reactive phase contained in both solid precursors used in this project. However, although the appearance of this hump on their X-ray patterns, some mineral peaks of hematite, quartz and maghemite, existing in both calcined solid precursors remain unaltered after alkaline activation. This suggests their non-participation into geopolymerization reaction.

By comparing the diffractograms of resulting geopolymers cured between 20 and 80 °C, it is observed the formation of newly formed crystalline mineral phases like siderite ($FeCO_3$, Sd, JCPDS N°. 29-696) and fayalite (Fe_2SiO_4, Fa, JCPDS N°. 34-178). Both solids precursors used in the present study are Fe-rich laterites and the iron minerals like hematite and maghemite in which the iron is in Fe^{3+} could be oxidized to Fe^{2+} in alkaline solution. When the reflection peaks of these iron mineral compounds decreased with increasing temperature from 20 to 80°C (X-ray diffractograms of geopolymers **Figure 5**). It appears some new crystalline mineral compounds containing iron such as Fayalite and siderite, which were detected in the geopolymer binders formed by XRD analysis. This suggests that a few amounts of these iron mineral phases contained in both solid precursors have reacted with silicate species to form fayalite and another one reacted with CO_2 from the atmosphere to form siderite. This quite matches the results of FTIR where the carbonate bands were attributed to the carbonation of Fe^{2+} and Na^+. Further details request Mossbauer spectroscopy which will be performed in the future in case an opportunity arises.

The more pronounced reflection peaks of fayalite formed in both geopolymer samples cured at 80°C are in line with previous works where the authors claimed that the iron silica compound is formed by a reaction involving iron mineral with dissolved silica at curing temperature of 50

to 200 °C [5,46]. Thus, using oven curing at 80 °C might cause a partial dissolution or alteration of iron minerals and then allowed the formation of fayalite which was more pronounced on these samples.

At variance, the formation of siderite at room temperature might be described by the fact that the formed mineral does not belong to the binding phase or exists as an isolated compound. Hence, the possible integration of iron atoms in a geopolymer network could be related to the instability of iron minerals in alkaline solution which seems to influence the oxidation of Fe^{2+} to Fe^{3+} [45]. Therefore, the non-incorporated Fe^{3+} (as non-geopolymer network forming) as unreacted Na^{+} could migrate out of the geopolymer matrix and could fix the CO_2 from the atmosphere as reported in previous work [30]. Nonetheless, further studies such as Mössbauer spectroscopy analysis can be carried out to have more understanding about the iron behaviour (i.e. in terms of coordination state) at this stage which is not the main target of the research conducted in this paper.

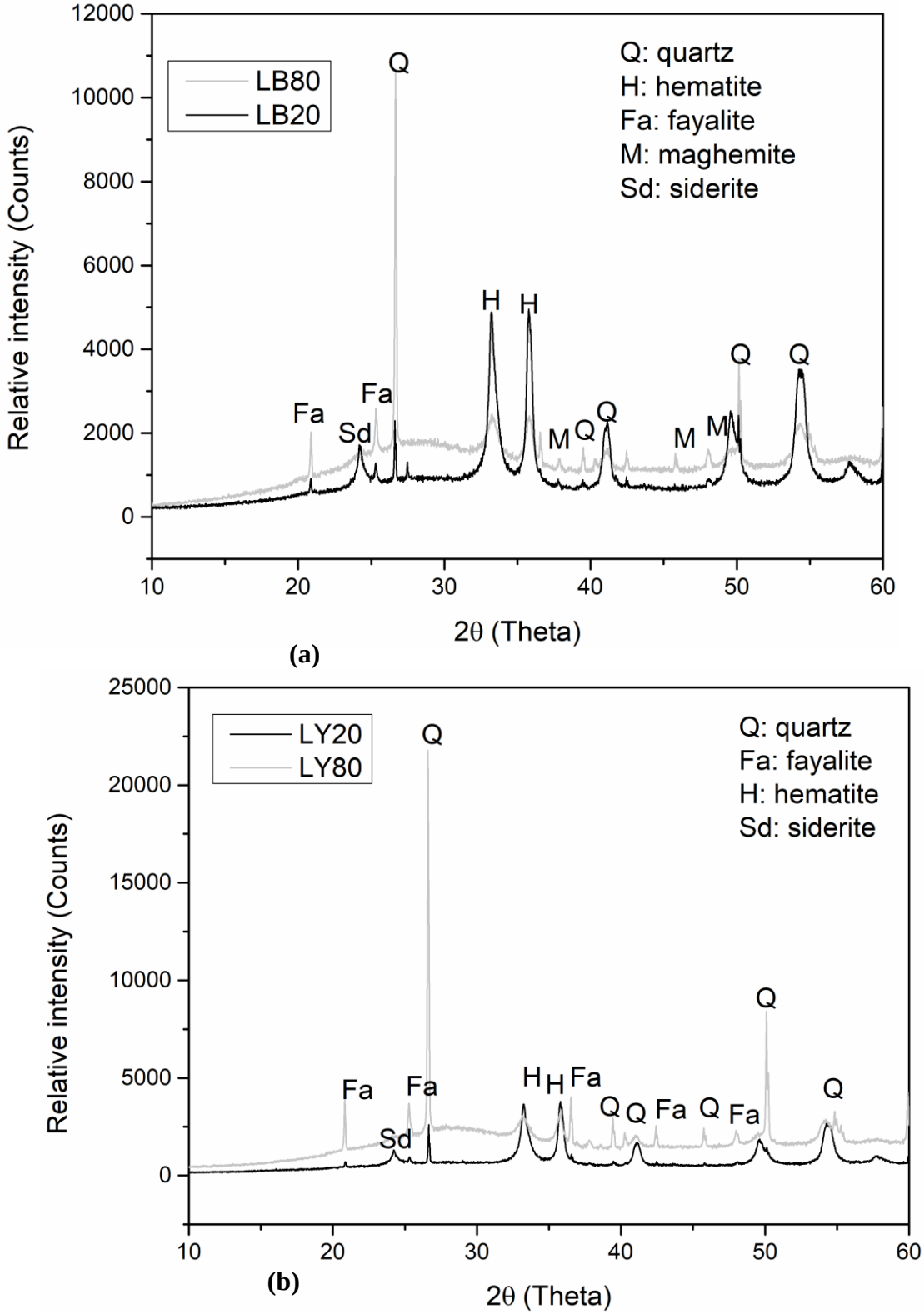

Figure 5 X-ray patterns of (**a**) LB20 and LB80 (**b**) LY20 and LY80

3.3.2 Compressive strength

3.3.2.1 Effect of curing temperature

The compressive strengths of both geopolymer series obtained from LB600 and LY600 are presented in **Figure 6**. From **Figure 6**, it is observed that the mechanical properties increased with the rise of temperature from 20 to 80°C and with curing age of 7 to 28 days. The values ranged between 18.10 to 28.90 MPa and 15.50 to 29.90 MPa respectively for geopolymer samples from LBi (i= 20, 60 and 80 °C) and LYi (i= 20, 60 and 80 °C) series cured at 7 days (**Figure 6a**). At 28 days, these values were 23.30 to 31.12 MPa and 25.24 to 32.20 MPa, respectively (**Figure 6b**).

Both calcined iron-rich laterites possess similar behaviour in strength development due to their similarity in mineralogical and chemical composition even though they have been harvested in two different localities in Cameroon far away from each other (i.e. 405 km apart). However, using oven curing during the synthesis had a positive effect on the mechanical performance of elaborated inorganic polymers (geopolymers). For example, increasing curing temperature from 20°C to 80 °C led to an improvement in mechanical strength.

The compressive strength of LB60 and LB80 is approximately 40 and 65% respectively, higher than that of LB20 at 7 days. Similarly, the compressive strength for LY60 and LY80 samples is approximately 44 and 92% respectively, higher than that of LY20 at 7 days. Whereas at 28 days, these values slightly increased between 11 to 29% and 14 to 34% for LYi(i= 20, 60 and 80°C) and LBi(i= 20, 60 and 80 °C) geopolymer series, respectively.

The increasing compressive strength with higher curing temperature can be ascribed to the rising rate of kinetic reaction and high dissolution of reactive phase (mainly metakaolin) contained in both solid precursors resulting in a high degree of geopolymerization leading to high polycondensation or polymerization between Si, Al and Fe species. This trend is also in line with the results of the dissolution of both calcined laterites explained earlier. Besides, the

elevated curing temperature at 60 and 80 °C used for the geopolymer binders allowed strength development during an early age (i.e. at 7 days). This suggests that the geopolymer matrix became more compact and denser by the initial curing at 60 and 80 °C for 2 hours, justifying the high strength gained on these samples. A similar trend has been reported in other studies where other aluminosilicates were used and increasing the curing temperature was found to improve the mechanical properties.

3.3.2.2 Effect of curing humidity

The values of wet compressive strength of both geopolymer series soaked after 48 h are also presented in **Figure 6**. It is well known in the literature that evaluation of the resistance to wet-dry cycles is an indication of the stability and durability of the binders [47]. After 48 h in distilled water, both geopolymers tend to lose their mechanical strength which decreased with higher curing temperature. The 28 days compressive strengths recorded on the samples subjected to wet curing ranged between 9.45 to 23.03 MPa and 19.45 to 26.92 MPa for geopolymer made with LB600 and LY600, respectively.

The losses in compressive strength at 28 days with augmentation of temperature decreased by 27 to 13% and 23 to 17% for geopolymer made with LB600 and LY600, respectively. The decrease in compressive recorded on samples immersed in water is linked to the integration of water molecules within the geopolymer network. This is due to the hydration of Si-O-Al and Si-O-Si bonds belonging to the geopolymer network leading to the formation of Silanol (Si-OH) and aluminol (Al-OH) bonds in the matrix which weakened the structure resulting in low strength achieved on these samples [13]. In addition, this reduction could be also related to the increase of the voids and pore size of the samples during immersion in water. Hence further investigations should be conducted to elucidate this hypothesis. Meanwhile, it is noticed although the fact that the geopolymer specimens were immersed in water during 48 h, they remain stable without visible fissures.

The residual compressive strength achieved at 28 days for all the samples is above 15 MPa justifying their use as a good cementitious material for building applications. The wet strengths achieved in both samples after immersion are higher than the strength obtained by Esaifan et al. [48] and Lemougna et al. [35] for alkali-activated kaolinitic clay and volcanic ash-based geopolymers, respectively where the authors recorded about 50 % of strength loss after immersion.

From **Figure 6**, it is observed that the soaked samples during 48 h after curing at 40 °C almost exceeded their wet compressive strength values. The 28 days compressive strengths of samples subjected to wet-dry state curing ranged between 12.56 to 25.03 MPa and 21.20-28.03 MPa when LB600 and LY600, respectively was used as the precursor. The oven curing at 40 °C of soaked samples for 48 h was chosen to avoid the abrupt evaporation which may cause the presence of cavities and fissures in the matrix that could be deleterious for strength development. These samples after the wet-dry curing period for 48 h gained reduced strength.

These results indicate the better stability of the binding phase formed in water with the rise of temperature from 20 to 80 °C. A similar trend was noticed on other aluminosilicates precursors (metakaolin, fly ash and volcanic ash) in geopolymer binder synthesis where an increase in strength was observed after immersion in water and oven curing of immersed samples [13,35,49].

In conclusion, higher curing temperature also enhances the compressive strength of samples subjected to a wet-dry state similar to those in the dry state. This indicates that oven curing between 60 and 80 °C appears as a key factor in the improvement of laterite based geopolymer binder properties and structural densification. In addition, the immersed samples after subsequent wetting-drying cycles gave higher strength (compared to wet strength recorded on soaked samples) almost similar to those in the dry state indicating that the binder phase formed was stable in water.

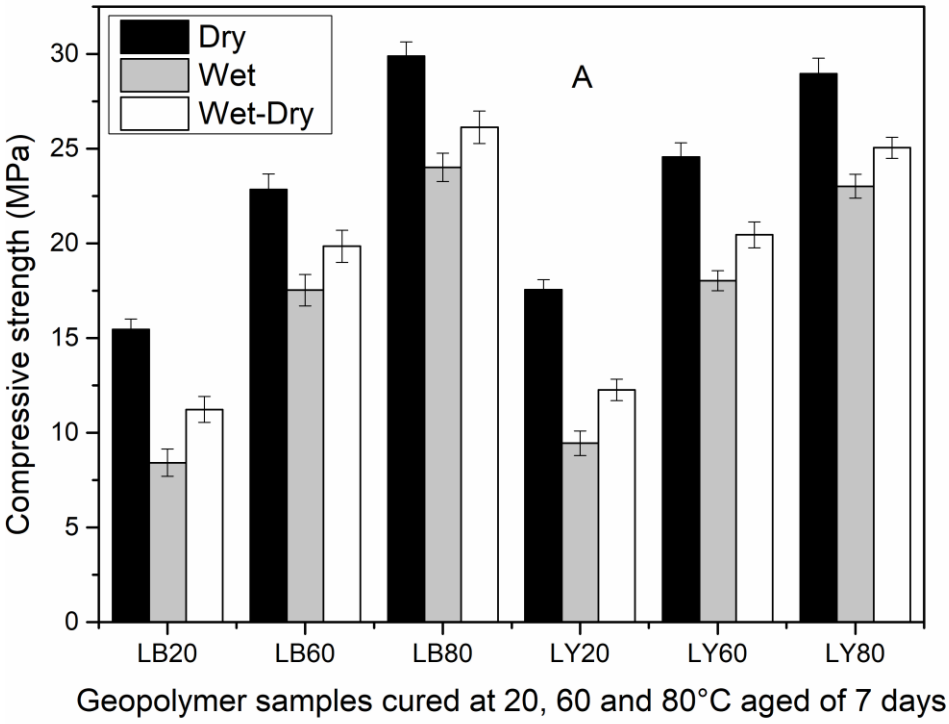

(a)

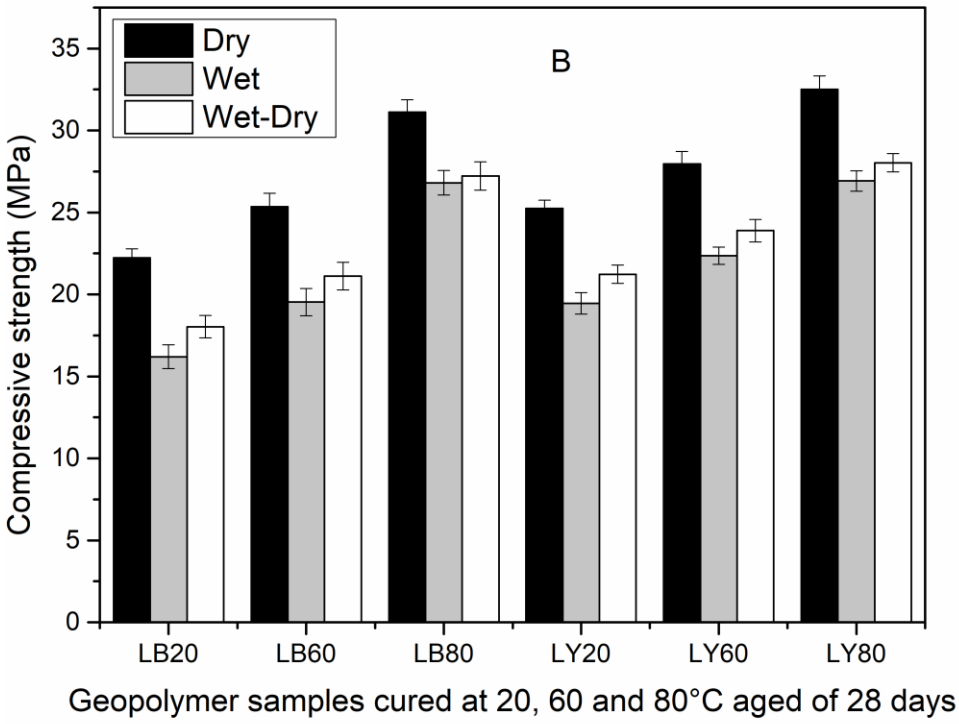

(b)

Figure 6 Compressive strength of geopolymer composites **(a)** 7 days **(b)** 28 days

3.3.3 Water absorption, porosity and bulk density

The water absorption, porosity and bulk density of the geopolymer binders are presented in **Figure 7**, **Figure 8** and **Figure 9**, respectively. From **Figure 7** it is evident that the water absorption decreased with the increase in temperature from 20 to 80 °C and also with curing age. The reduction in water absorption is consistent with the trend observed for mechanical properties. The compact and dense structure only retained low water when immersed in water for water absorption and porosity test. With the rise of temperature from 20 to 80 °C, the values of porosity (**Figure 8**) decreased from 29% to 20 % and 27 to 16 % for geopolymer made with LB600 and LY600, respectively. The reduction in porosity (**Figure 8**) can be attributed to the increase in curing temperature which results in the higher dissolution of the reactive phase leading to an important polymerization and densification of the geopolymer matrix.

The bulk density values of both resulting geopolymers are presented in **Figure 9**. From **Figure 9**, it is seen that the bulk density decreased at 7 days at different curing regimes but remained almost the same at 28 days. The decrease in bulk density observed on wet and wet-dry samples could be ascribed to the fact that during the immersion, some unreacted particles could have leached out of the matrix, making the samples lighter. Whereas the increase in bulk density with curing temperature can be attributed to the presence of a lower number of voids in the matrix due to the extended geopolymer structure. Thus, the geopolymer network became more compact due to well adhesion and cohesion among different components in the matrix which makes them denser. The bulk density development correlates with the compressive strength results.

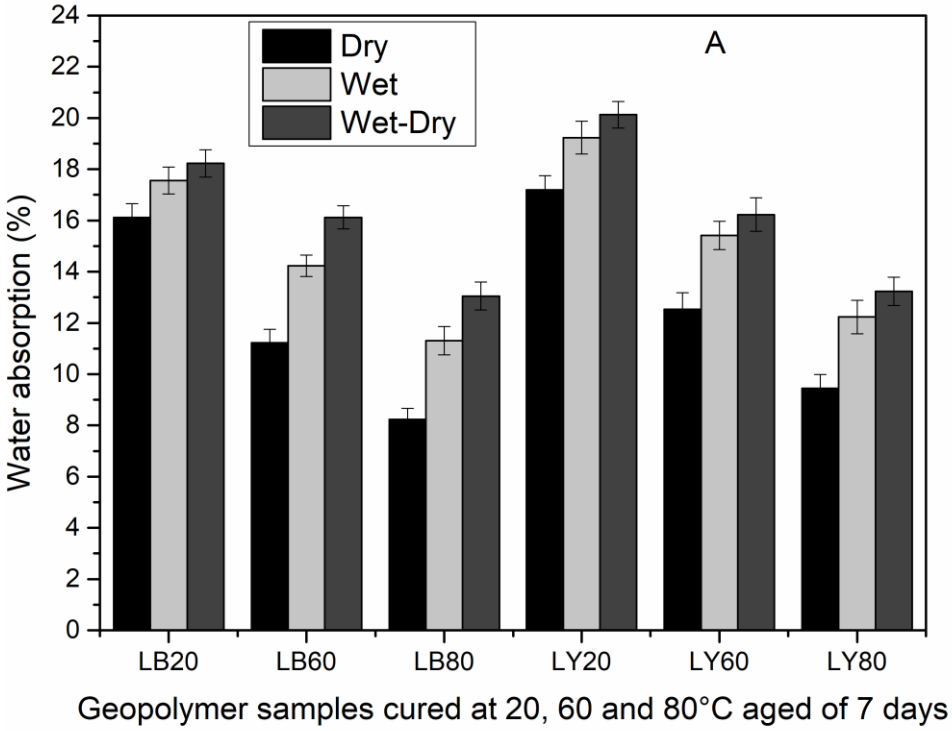

(a)

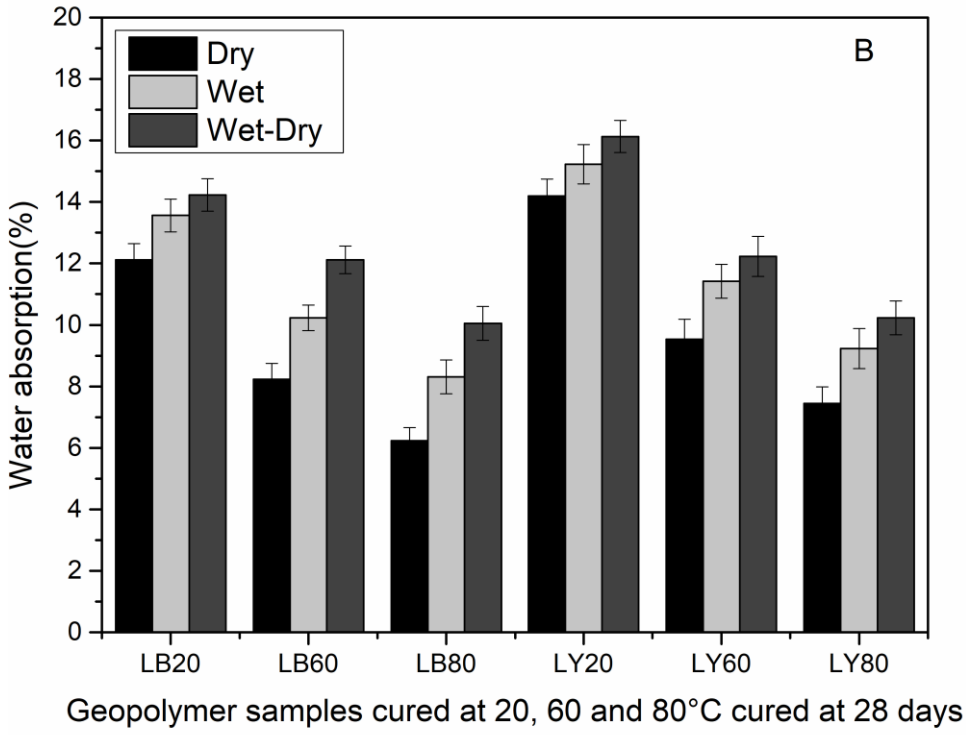

(b)

Figure 7 Water absorption of geopolymer composites **(a)** 7 days **(b)** 28 days

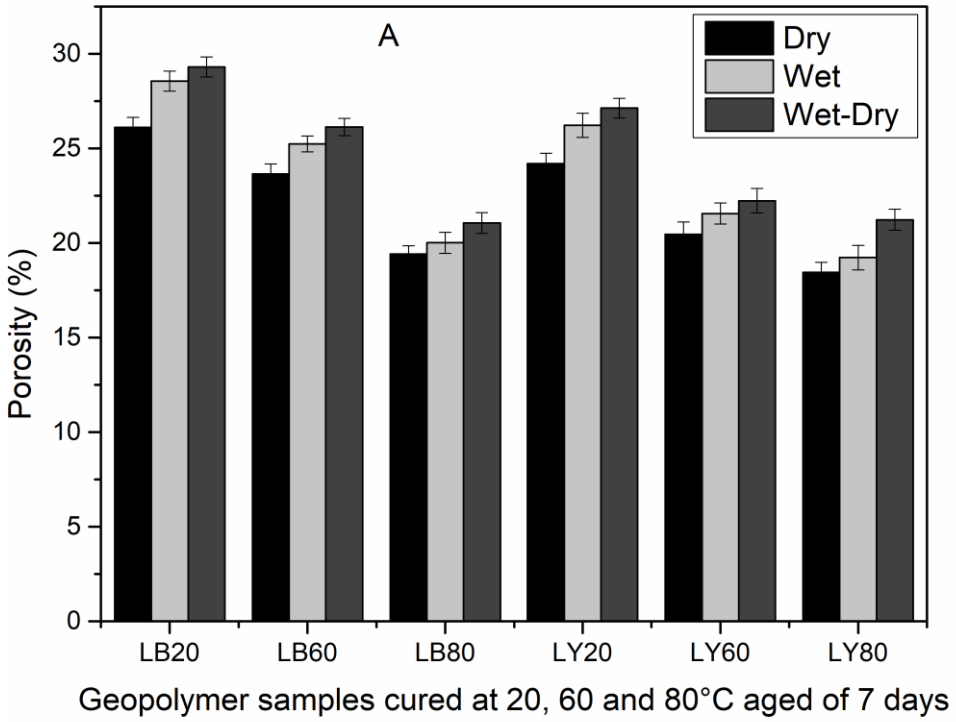

(a)

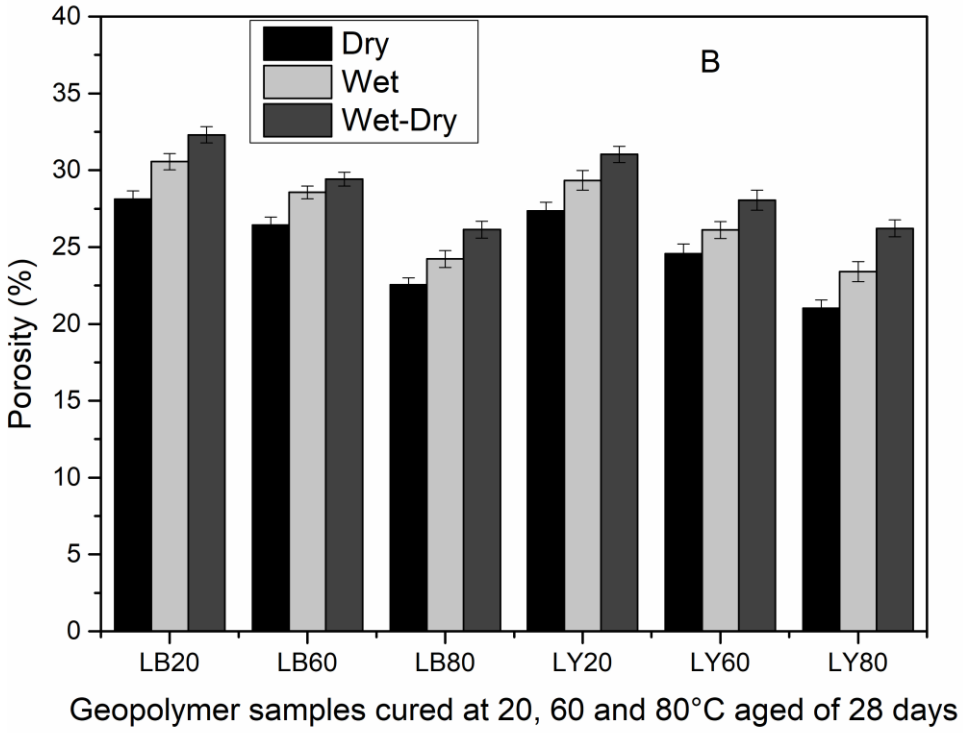

(b)

Figure 8 Porosity of geopolymer composites **(a)** 7 days **(b)** 28 days

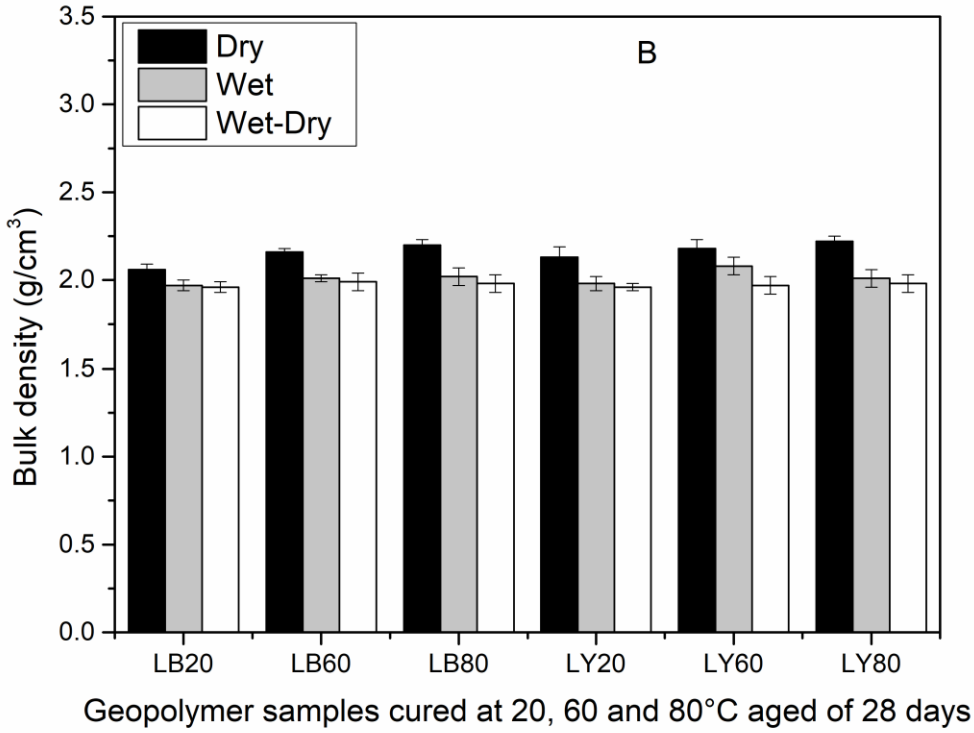

(a)

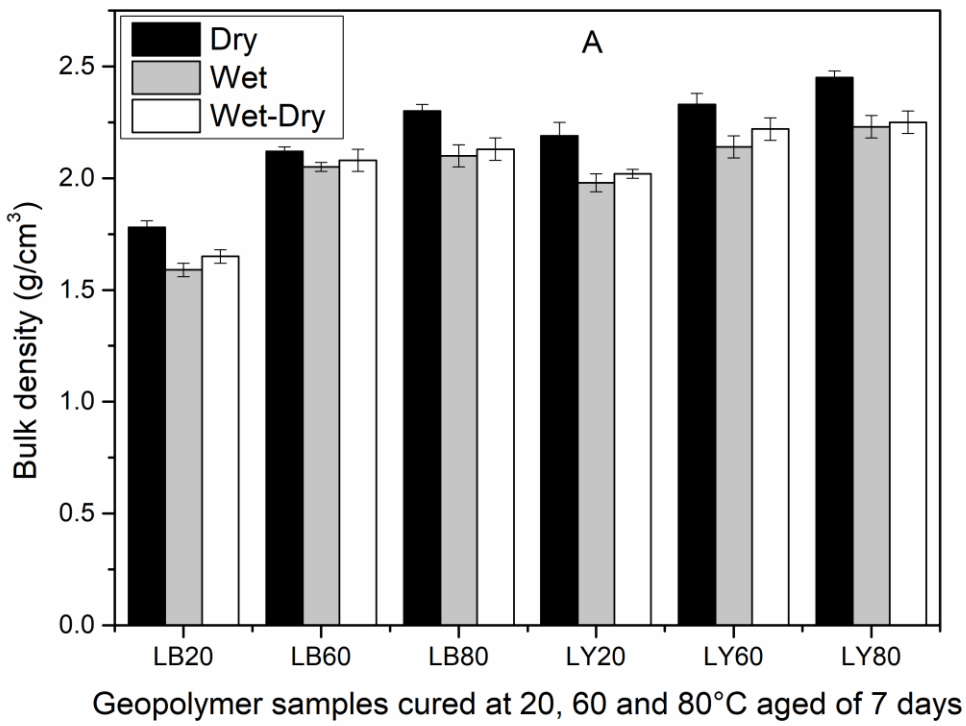

(b)

Figure 9 Bulk density of geopolymer composites **(a)** 7 days **(b)** 28 days

3.3.4 Drying shrinkage

The drying shrinkages observed for the geopolymer samples at 7, 14, 21 and 28 days are tabulated in **Table 4**. It is can be seen from **Table 4** that the drying shrinkage of the samples reduced with higher temperatures and increased with age. The reduction in the drying shrinkage with higher temperatures could be justified by the fact that during the synthesis, the oven curing favoured the high dissolution of the reactive phase resulting in a high degree of polymerization. As a result of the higher degree of polymerization, more binding phases were formed and embedded into a matrix followed by high consumption of water. The high consumption of the free water will prevent the evaporation of water out of the matrix which can result in a decrease in length with time.

The comparable tendency had been observed by Ridtirud et al. [50] and Gorhan et al. [51] who concluded that a compact or dense geopolymer network with low shrinkages can be produced at a temperature beyond the room temperature curing. This is related to the improvement of kinetic reaction that induced the most leaching of geopolymer ingredients like Al, Fe and Si in alkaline medium related to a high degree of geopolymerization. However, the high shrinkage values recorded on both geopolymer LB20 and LY20 samples cured at room temperature (20 °C) might be linked to non-reactive or unfixed sodium ions and water molecules that diffused or migrated out of geopolymer matrix producing the reduction size [11].

Table 4. Drying shrinkage (%) of geopolymer binders from both calcined laterites cured at 7, 14, 21 and 28 days.

Geopolymer samples	**7 days**	**14 days**	**21 days**	**28 days**
LB20	0.41±0.02	0.61±0.02	0.65±0.02	0.65±0.02
LB60	0.32±0.02	0.38±0.02	0.41±0.02	0.40±0.02
LB80	0.24±0.02	0.28±0.02	0.30±0.02	0.30±0.02
LY20	0.52±0.02	0.65±0.02	0.68±0.02	0.69±0.02
LY60	0.43±0.02	0.49±0.02	0.50±0.02	0.50±0.02
LY80	0.32±0.02	0.36±0.02	0.37±0.02	0.37±0.02

3.3.5 Microstructure

The SEM images exhibiting in detail the morphological structure of geopolymer LB20, LB80, LY20 and LY80 samples at different magnifications are presented in **Figures 10**. For the geopolymer LB20 and LY20 cured at room temperature (**Figures 10a** and **Figure 10b**), the micrographs appear heterogeneous and less dense than those recorded at higher curing temperatures, exhibiting fissures, voids and poor cohesion between particles. The presence of these voids could be either due to the water evaporation during drying time which occupied the cavities or non-sufficient formation of geopolymer binder necessary for well adhesion or agglomeration between different constituents in the matrix. Thus, the appearance of fissures and voids is responsible for the low strength gained on these samples.

The SEM images of geopolymer LB80 and LY80 samples (**Figure 10c** and **Figure 10d**) presented a strong compact and dense structure with lower heterogeneity due to the higher formation of the geopolymer products. More precisely, the rise of curing temperature during the geopolymerization allowed the formation of Na-polysialate (Si-O-Al) and Na-polyferrosialate (Si-O-(Fe)Al) binder types in alkaline medium, resulting from the dissolution of reactive phase (containing Al, Si and Fe compounds) that allowed development of compact structure justifying the improvement in mechanical performance. This tendency is in line with that of reactivity test and mechanical performances.

The chemical compositions of geopolymer binder in both geopolymer samples LB80 and LY80 cured at 80 °C calculated from EDS analysis are presented in **Tables 5 and 6.** As seen from Tables 5 and 6; Na, O, Si, Al and Fe appear as major elements. For LB80 sample, the chemical composition in molar ratios of Si/Al = 1.22-3.00, Si/Fe = 0.13-1.00, Na/Al = 0.14-0.41 and Na/Fe = 0.01-0.20 are reported in **Table 5** and **Figure 11a**. For LY80, Si/Al = 1.30-1.81, Si/Fe = 0.15-1.80, Na/Al = 0.20-0.70 and Na/Fe = 0.10-0.90 are reported in **Table 6** and **Figure 11b**. These chemical compositions in both geopolymer LB80 and LY80 specimens are attributed to

amorphous Na-polyferrosialate and Na-polyferrosialate-multisiloxo geopolymer binder types as reported previously by other authors. This observation corresponds to other studies where different iron-rich aluminosilicates precursors were used for geopolymer synthesis [5,11]. From the Na/Si and Na/Fe molar ratios reported in **Tables 5 and 6**, it could be expected that some iron leached during the dissolution were incorporated into a geopolymer network and limited the accessibility of free sodium [52]. This hypothesis quite matches with the lower intensity of C-O bonds exhibited in the FTIR spectra recorded on these samples. This suggests that some iron could act as a network modifier even though further analysis like Mössbauer needs to be conducted for a better explanation.

According to findings of Davidovits and Davidovits [3] the calcination of kaolin containing iron compounds like goethite and magnetite heating between 600 and 800 °C are transformed to Ferro-metakaolin showing the substitution of Al^{3+} by Fe^{3+} allowing the formation of Na polyferrosialate (-Fe-O-Si-O-Al-O-) binder confirmed by ^{57}Fe Mössbauer spectroscopy analysis.

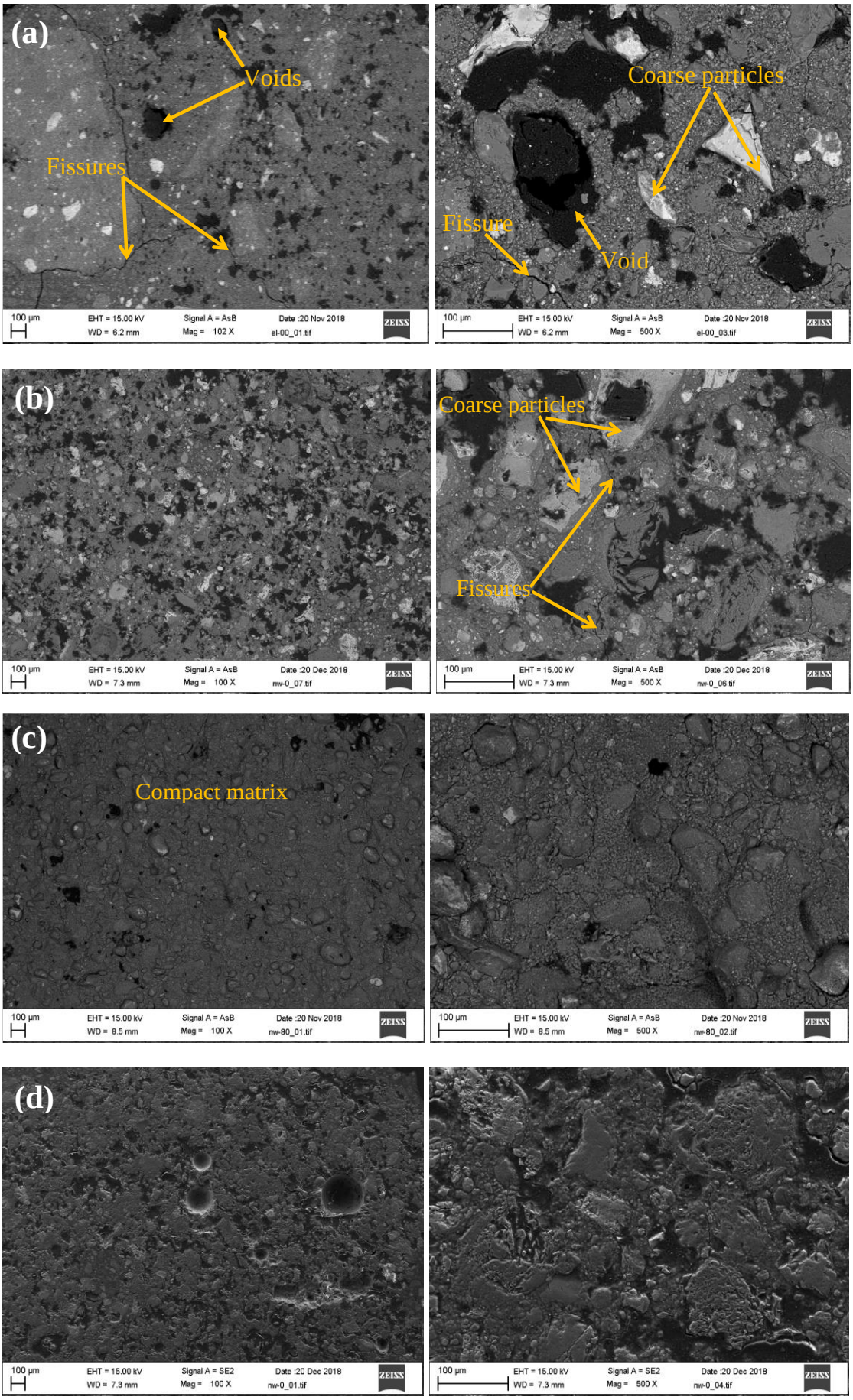

Figure 10 SEM images **(a)** LB20 **(b)** LY20 **(c)** LB80 **(d)** LY80

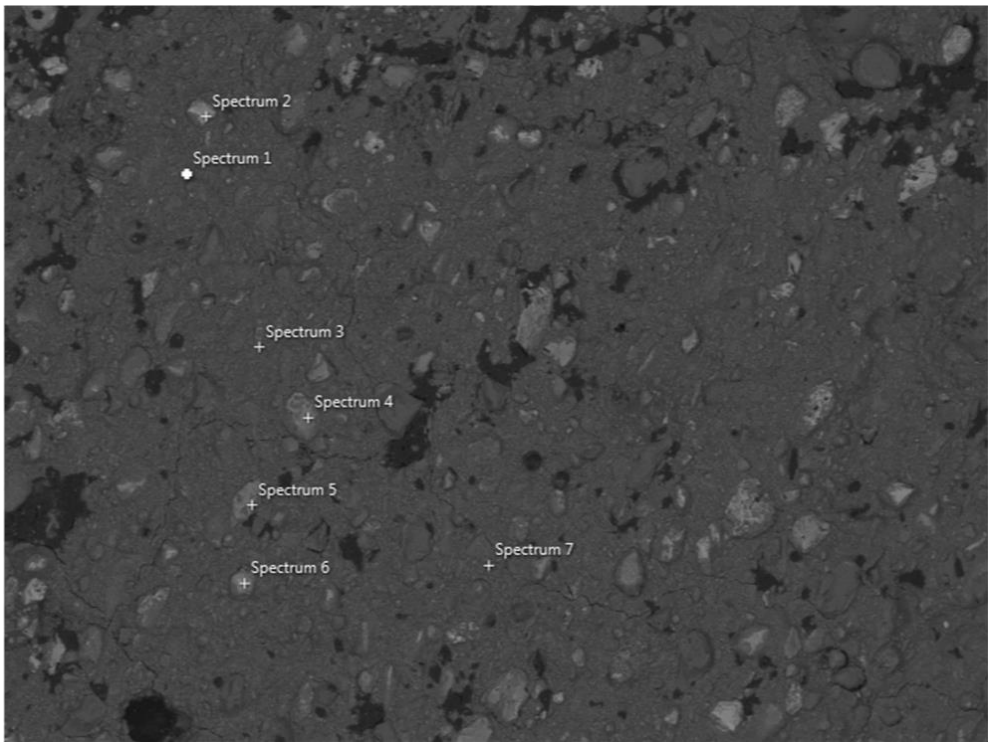

(a)

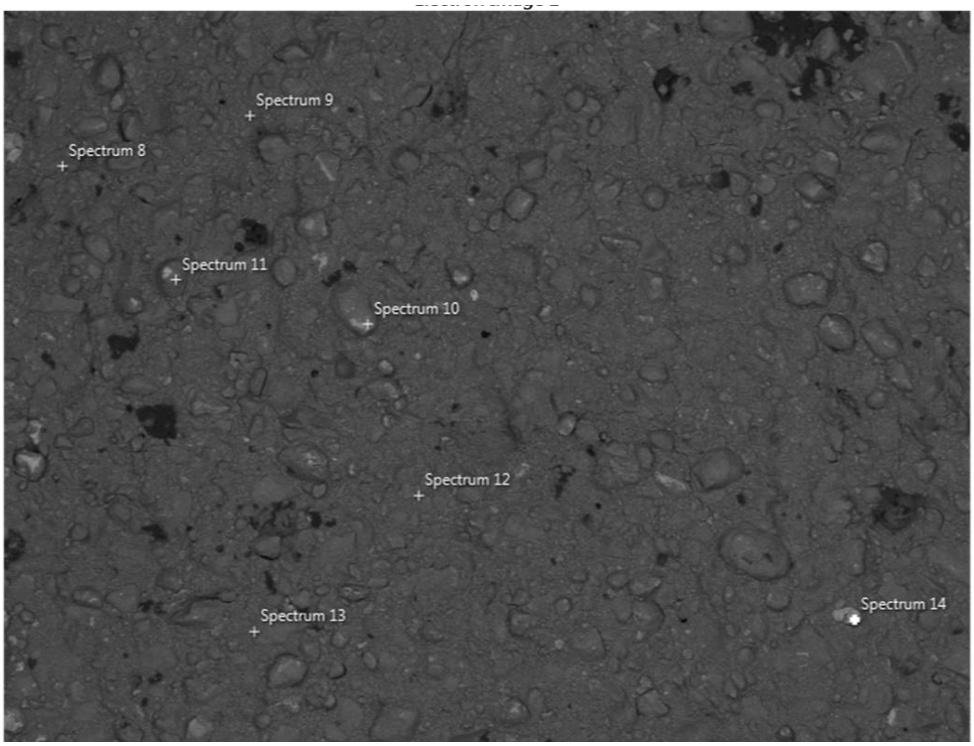

(b)

Figure 11 Points selected for EDS analysis **(a)** LB80 **(b)** LY80

Table 5. Elemental analysis from EDS of geopolymer LB80 sample.

Concentration of elements (wt %)	Spectrum 1	Spectrum 2	Spectrum 3	Spectrum 4	Spectrum 5	Spectrum 6	Spectrum 7
O	35.80	2.80	23.80	41.10	20.20	32.30	3.00
Si	15.00	22.00	26.20	16.00	10.70	4.20	9.30
Al	11.90	7.40	16.30	13.10	7.30	7.70	4.90
Fe	32.00	59.50	26.40	25.50	43.50	53.50	73.00
Na	4.90	1.60	6.00	2.10	1.90	1.50	0.7
Si/Al	1.26	2.97	1.61	1.22	1.46	0.54	1.89
Si/Fe	0.47	0.37	0.99	0.63	0.25	0.08	0.13
Na/Al	0.41	0.23	0.34	0.16	0.26	0.40	0.14
Na/Fe	0.15	0.03	0.22	0.08	0.04	0.03	0.01

Table 6. Elemental analysis from EDS of geopolymer LY80 sample.

Concentration of elements (wt %)	Spectrum 8	Spectrum 9	Spectrum 10	Spectrum 11	Spectrum 12	Spectrum 13	Spectrum 14
O	46.30	19.00	36.30	30.70	41.30	48.00	34.80
Si	18.30	18.20	7.80	21.30	13.10	17.30	7.00
Al	13.30	10.10	11.30	15.00	10.20	11.70	6.10
Fe	10.20	37.00	42.40	25.10	28.30	11.10	46.60
Na	9.10	3.70	2.30	2.50	4.4	7.50	3.80
Si/Al	1.38	1.81	0.70	1.42	1.30	1.50	0.15
Si/Fe	1.79	0.50	0.18	0.84	0.46	1.56	0.15
Na/Al	0.70	0.40	0.20	0.17	0.43	0.64	0.63
Na/Fe	0.89	0.05	0.10	0.15	0.68	0.08	0.63

3.3.6 Thermal conductivity measurements (λ, W/mK)

The thermal conductivity values recorded for the geopolymer samples are presented in **Figure 12**. It can be observed from the figure that the thermal conductivity increased with the increase in temperature from 20 to 80 °C. The low values of 0.58 and 0.69 W/mK recorded on LB20 and LY20 samples, respectively, are directly linked to their porous microstructure from SEM analysis (**Figures 10a** and **Figure 10b**). The presence of voids and fissures in these samples will affect the rate of diffusion of heat transfer through the samples during the measurements

[52,53]. The high thermal conductivity of samples oven-cured between 60 and 80 °C can be related to good cohesion between the binding phase and different particles. However, the iron content present in both solid precursors (i.e. LB600 and LY600) also contributes to the higher thermal conductivity. It is noticed that both starting materials used as main materials for geopolymer synthesis are ferruginous soils.

Hence, the good distribution of iron mineral compounds across the geopolymer matrix would enable the high diffusion of heat that resulted in high thermal conductivity values. Hence, laterite geopolymer binder cured at room temperature can be used for construction applications such as building envelops where low thermal conductivity is desired. The geopolymer cured at elevated temperatures (i.e. 60 and 80 °C) can be used for construction applications where higher thermal conductivity is required. The correlation between the densification of geopolymer matrix and thermal conductivity has also been stated by Kamseu et al. [54] and Novais et al. [55] on metakaolin and porous fly ash-based geopolymers, respectively.

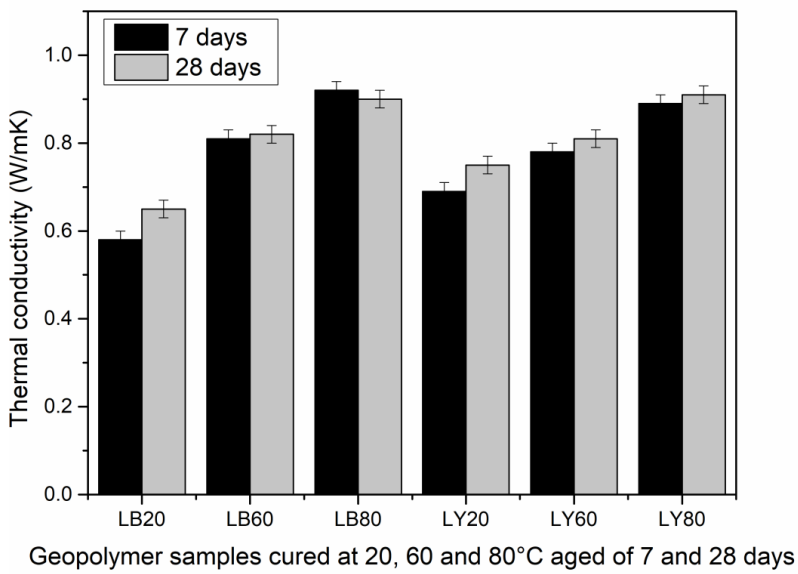

Figure 12 Thermal conductivity of geopolymer binders

3.3.7 Thermal behaviour (TG/DTA)

The simultaneous TG/DTA analyses of selected geopolymer samples made from LB600 and LY600 are presented in **Figure 13** and **Figure 14** respectively. This analysis is well known to study the behaviour of newly formed mineral phases in cementitious materials under high temperatures. The less pronounced endothermic peaks that appear near 100 °C in LB20 and LY20 samples are due to the departure of free or physiosorbed water (**Figure 13a** and **Figure 14a**). This has been previously reported by published works focused on alkali-activated binders [19,56]. This is accompanied by a lower weight loss of less than 1 % recorded on TG curves.

However, the more pronounced endothermic peaks around 150 °C for all the specimens are linked to the evaporation of structural or chemical water molecules belonging to the geopolymer network [57]. This is due to the destruction of chemical bonds of Si-O-Al, Si-O-Fe and Si-O-Si belonging to geopolymer structure. In the given study it is not observed any endothermic peak above 150°C in DTA curves of all the geopolymer formed without any loss in weight in TG curves. This could be justified by the fact both calcined laterites did not contain any trace of hydroxylated compounds. Thus at 600 °C, all kaolinite mineral presents in both raw iron-rich laterites were totally transformed into metakaolinite. In addition, the almost none important observed endothermic peaks after 200 °C could be due to low content of solid/liquid ratio of 0.6 compared to that of metakaolin based geopolymer that generally ranged between 0.7and 1. Therefore the calcined iron-rich laterite would not adopt the same behaviour during the thermal

analysis like metakaolin based geopolymer.

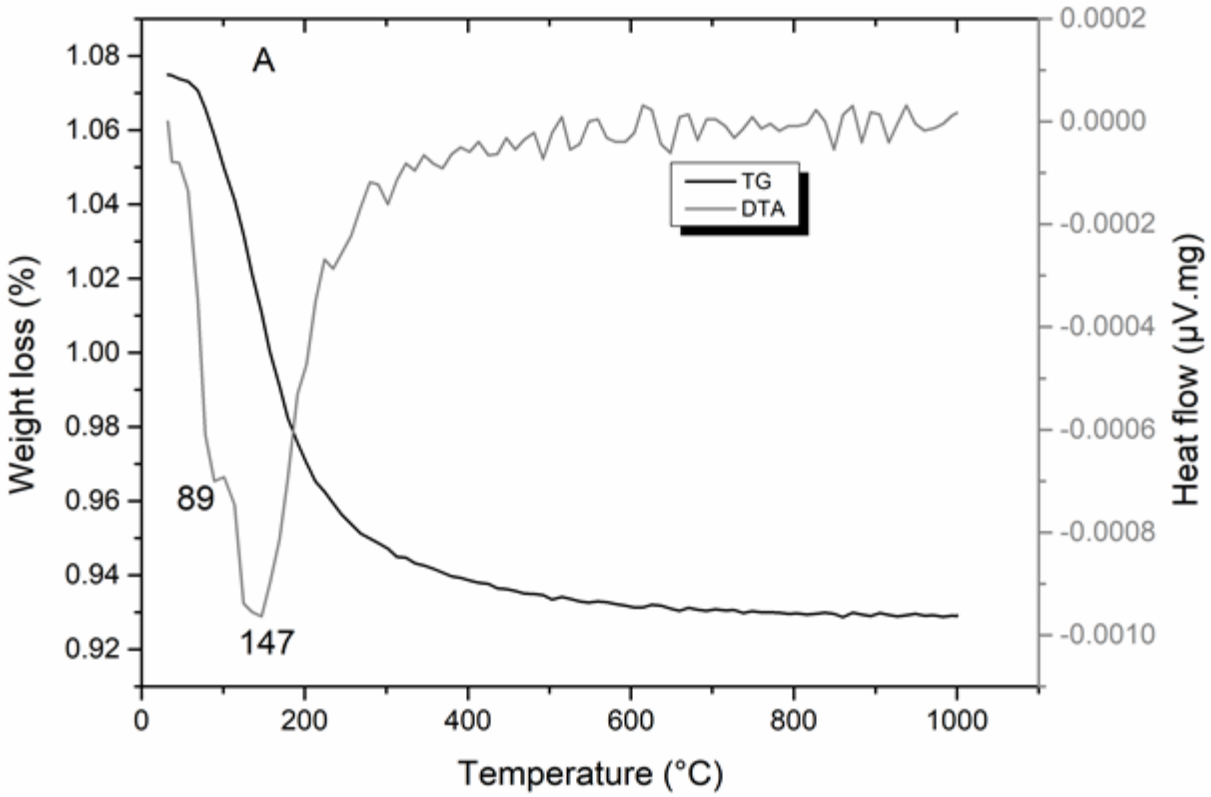

(a)

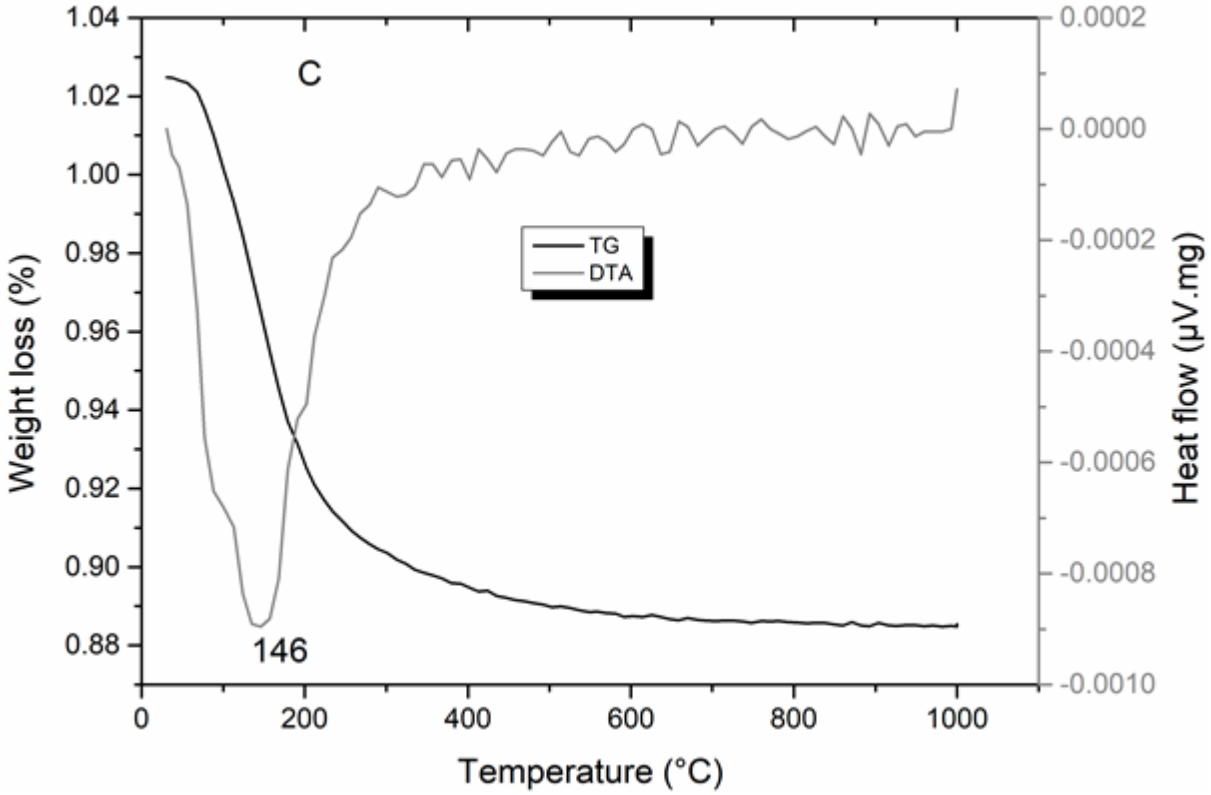

(b)

Figure 13 DTA/TG curves of consolidated geopolymer **(a)** LB20 **(b)** LB80

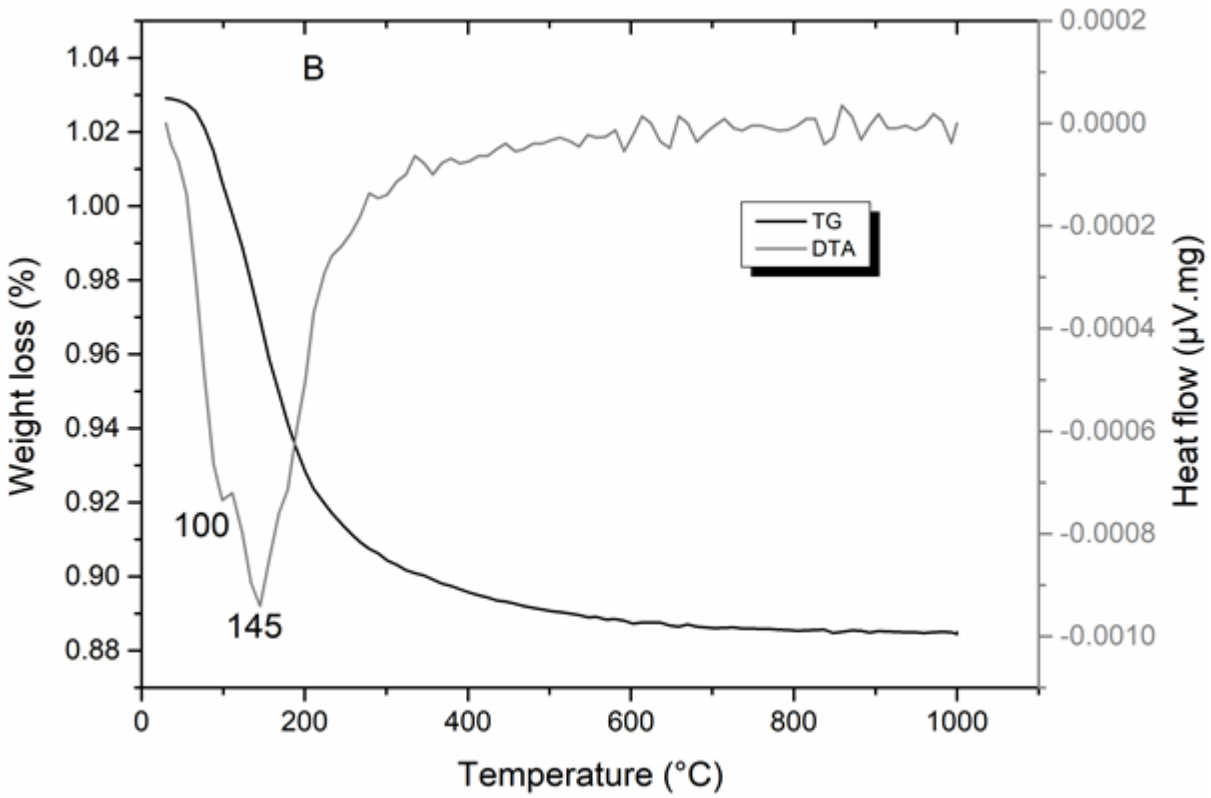

(a)

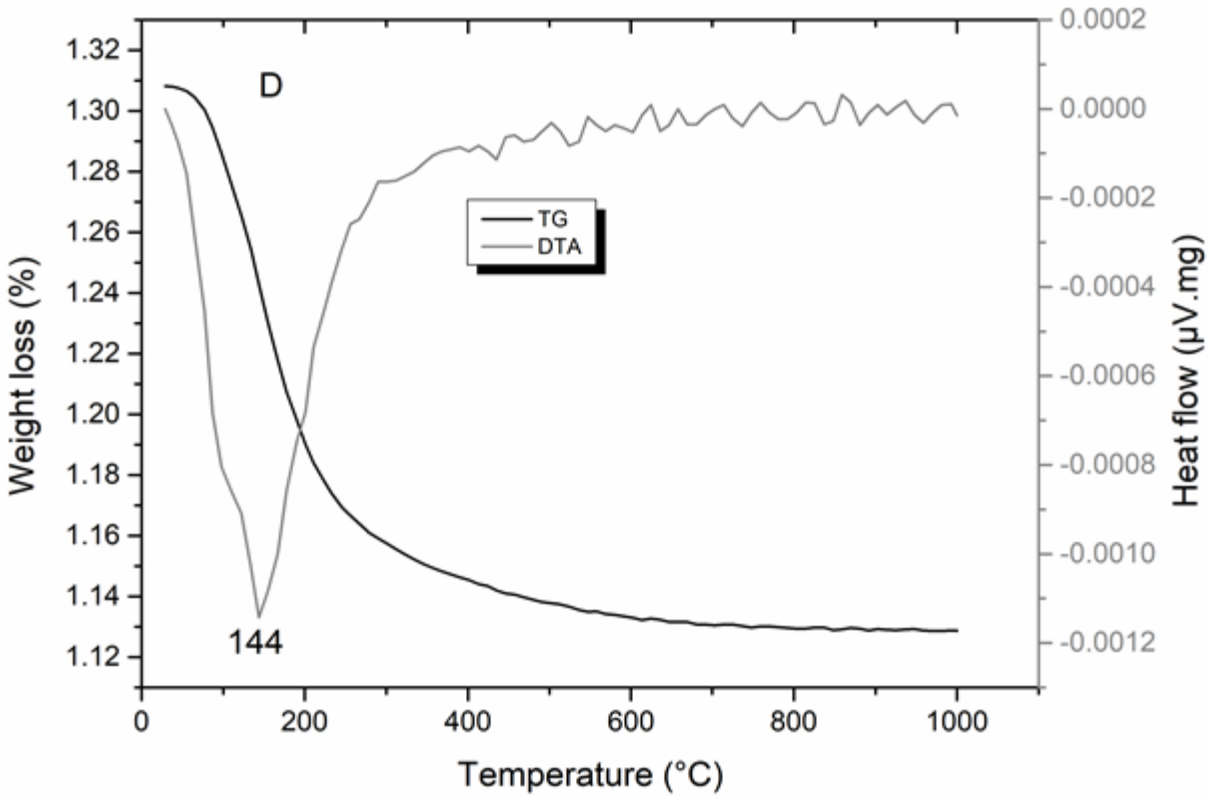

(b)

Figure 14 DTA/TG curves of consolidated geopolymer **(a)** LY20 **(b)** LY80

4. Conclusion

This current study evaluated the effect of curing temperature (i.e. 20, 60 and 80 °C) on microstructural and physical properties as well as thermal conductivity, porosity, bulk density and water absorption of geopolymer binders prepared from two calcined iron-rich laterites (LB600 and LY600). The tests were conducted on geopolymer samples resulting from both laterites. Based on the outcome of this study, the following conclusions can be drawn:

1. Increasing curing temperature from 20 to 80 °C enhanced the solubility of Al, Si and Fe elements and induced an extension of geopolymer network which improved the mechanical properties of dry specimens leading to a high degree of polymerization that contributed to densify the geopolymer structure;
2. SEM/EDS analysis pointed out the micrographs of geopolymer samples exhibiting the amorphous Na-poly(ferrosialate) and Na-(polyferrosialate-multisiloxo) as the main binder phases responsible for the strength development in both geopolymer series;
3. The increase in thermal conductivity and bulk density was linked to well cohesion or connectivity between geopolymer binder and other particles which reduced the formation of the voids within the matrix;
4. The reduction in compressive strength of soaked samples in water after 48 h was due to formed Si-OH or Al-OH bonds due to hydration phenomenon which became less sturdy in the matrix and leads to decrease in mechanical strength development;
5. The end products were stable in water after wetting-drying cycles with mechanical performance > 15 MPa allowing these synthesized materials to be considered as potential materials construction such as road pavement, buildings etc.

Acknowledgements

This project received the contribution of the FLAIR fellowship African Academic of Science and the Royal Society through the funding N° FLR/R1/201402. The authors also are grateful to Ingessil S.r.l., Verona, Italy, for providing sodium silicate used. RCK grateful acknowledges the financial support of AVRUL (Agence pour la Valorisation de la Recherche Universitaire du Limousin) for his stay in IRCER, UMRCNRS 7315, Limoges under 2018 AVRUL postgraduate internship. PNL is acknowledging the support from the Fibre and Particle Engineering Research Unit, University of Oulu, Finland.

References

[1] C.N. Bewa, H.K. Tchakouté, C.H. Rüscher, E. Kamseu, C. Leonelli, Influence of the curing temperature on the properties of poly(phospho-ferro-siloxo) networks from laterite, SN Appl. Sci. (2019). https://doi.org/10.1007/s42452-019-0975-5.

[2] J. Davidovits, Geopolymers - Inorganic polymeric new materials, J. Therm. Anal. (1991). https://doi.org/10.1007/BF01912193.

[3] J. Davidovits, R. Davidovits, Ferro-sialate Geopolymers (-Fe-O-Si-O-Al-O-) Geopolymer Institute Library Ferro-sialate Geopolymers (-Fe-O-Si-O-Al-O-), (2020). https://doi.org/10.13140/RG.2.2.25792.89608/2.

[4] J.N.Y. Djobo, H.K. Tchakouté, N. Ranjbar, A. Elimbi, L.N. Tchadjié, D. Njopwouo, J. Biernacki, Gel Composition and Strength Properties of Alkali-Activated Oyster Shell-Volcanic Ash: Effect of Synthesis Conditions, J. Am. Ceram. Soc. (2016). https://doi.org/10.1111/jace.14332.

[5] E. Kamseu, C.R. Kaze, J.N.N. Fekoua, U.C. Melo, S. Rossignol, C. Leonelli, Ferrisilicates formation during the geopolymerization of natural Fe-rich aluminosilicate precursors, Mater. Chem. Phys. (2020).

https://doi.org/10.1016/j.matchemphys.2019.122062.

[6] R.C. Kaze, L.M. Beleuk à Moungam, M. Cannio, R. Rosa, E. Kamseu, U.C. Melo, C. Leonelli, Microstructure and engineering properties of Fe2O3(FeO)-Al2O3-SiO2 based geopolymer composites, J. Clean. Prod. (2018). https://doi.org/10.1016/j.jclepro.2018.07.171.

[7] H.K. Tchakouté, S.J.K. Melele, A.T. Djamen, C.R. Kaze, E. Kamseu, C.N.P. Nanseu, C. Leonelli, C.H. Rüscher, Microstructural and mechanical properties of poly(sialate-siloxo) networks obtained using metakaolins from kaolin and halloysite as aluminosilicate sources: A comparative study, Appl. Clay Sci. (2020). https://doi.org/10.1016/j.clay.2020.105448.

[8] A.G. Mimboe, M.T. Abo, J.N.Y. Djobo, S. Tome, R.C. Kaze, J.G.N. Deutou, Lateritic soil based-compressed earth bricks stabilized with phosphate binder, J. Build. Eng. (2020). https://doi.org/10.1016/j.jobe.2020.101465.

[9] K. Cyriaque, L. LAURE, K. Elie, C. Uphie, STUDY OF THE CONSOLIDATION OF LATERITE THROUGH ORGANIC AND INORGANIC ACIDS, Pubs.Ub.Ro. (n.d.). http://pubs.ub.ro/dwnl.php?id=PLUMEE201901V09S01A0021 (accessed May 29, 2020).

[10] H.K. Tchakouté, C.H. Rüscher, E. Kamseu, F. Andreola, C. Leonelli, Influence of the molar concentration of phosphoric acid solution on the properties of metakaolin-phosphate-based geopolymer cements, Appl. Clay Sci. (2017). https://doi.org/10.1016/j.clay.2017.07.036.

[11] C.R. Kaze, P. Venyite, A. Nana, D.N. Juvenal, H.K. Tchakoute, H. Rahier, E. Kamseu, U.C. Melo, C. Leonelli, Meta-halloysite to improve compactness in iron-rich laterite-based alkali activated materials, Mater. Chem. Phys. (2020).

https://doi.org/10.1016/j.matchemphys.2019.122268.

[12] O. Aluko, T. Awolusi, A. Adesina, Influence of Curing Media and Mixing Solution on the Compressive Strength of Laterized Concrete, Silicon. (2019). https://doi.org/10.1007/s12633-019-00343-x.

[13] P.N. Lemougna, A.B. Madi, E. Kamseu, U.C. Melo, M.P. Delplancke, H. Rahier, Influence of the processing temperature on the compressive strength of Na activated lateritic soil for building applications, Constr. Build. Mater. (2014). https://doi.org/10.1016/j.conbuildmat.2014.04.100.

[14] P.N. Lemougna, K. tuo Wang, Q. Tang, E. Kamseu, N. Billong, U. Chinje Melo, X. min Cui, Effect of slag and calcium carbonate addition on the development of geopolymer from indurated laterite, Appl. Clay Sci. (2017). https://doi.org/10.1016/j.clay.2017.08.015.

[15] C.R. Kaze, J.N.Y. Djobo, A. Nana, H.K. Tchakoute, E. Kamseu, U.C. Melo, C. Leonelli, H. Rahier, Effect of silicate modulus on the setting, mechanical strength and microstructure of iron-rich aluminosilicate (laterite) based-geopolymer cured at room temperature, Ceram. Int. (2018). https://doi.org/10.1016/j.ceramint.2018.08.205.

[16] R.C. Poudeu, C.J. Ekani, C.N. Djangang, P. Blanchart, Role of heat-treated laterite on the strengthening of geopolymer designed with laterite as solid precursor, Ann. Chim. Sci. Des Mater. (2019). https://doi.org/10.18280/acsm.430601.

[17] B. Singh, G. Ishwarya, M. Gupta, S.K. Bhattacharyya, Geopolymer concrete: A review of some recent developments, Constr. Build. Mater. (2015). https://doi.org/10.1016/j.conbuildmat.2015.03.036.

[18] O.A. Abdulkareem, A.M. Mustafa Al Bakri, H. Kamarudin, I. Khairul Nizar, A.A. Saif,

Effects of elevated temperatures on the thermal behavior and mechanical performance of fly ash geopolymer paste, mortar and lightweight concrete, Constr. Build. Mater. (2014). https://doi.org/10.1016/j.conbuildmat.2013.09.047.

[19] M. Youmoue, R.T. Tene Fongang, A. Gharzouni, R.C. Kaze, E. Kamseu, V.M. Sglavo, I. Tonle Kenfack, B. Nait-Ali, S. Rossignol, Effect of silica and lignocellulosic additives on the formation and the distribution of meso and macropores in foam metakaolin-based geopolymer filters for dyes and wastewater filtration, SN Appl. Sci. (2020). https://doi.org/10.1007/s42452-020-2388-x.

[20] A. Adesina, Performance of fibre reinforced alkali-activated composites – A review, Materialia. 12 (2020) 100782. https://doi.org/10.1016/j.mtla.2020.100782.

[21] A.A. Adam, Horianto, The effect of temperature and duration of curing on the strength of fly ash based geopolymer mortar, in: Procedia Eng., 2014. https://doi.org/10.1016/j.proeng.2014.12.199.

[22] T. Bakharev, Thermal behaviour of geopolymers prepared using class F fly ash and elevated temperature curing, Cem. Concr. Res. (2006). https://doi.org/10.1016/j.cemconres.2006.03.022.

[23] H. Cheng-Yong, L. Yun-Ming, M.M.A.B. Abdullah, K. Hussin, Thermal Resistance Variations of Fly Ash Geopolymers: Foaming Responses, Sci. Rep. (2017). https://doi.org/10.1038/srep45355.

[24] J.N.Y. Djobo, A. Elimbi, H.K. Tchakouté, S. Kumar, Reactivity of volcanic ash in alkaline medium, microstructural and strength characteristics of resulting geopolymers under different synthesis conditions, J. Mater. Sci. (2016). https://doi.org/10.1007/s10853-016-0257-1.

[25] P.N. Lemougna, K.J.D. MacKenzie, U.F.C. Melo, Synthesis and thermal properties of inorganic polymers (geopolymers) for structural and refractory applications from volcanic ash, Ceram. Int. (2011). https://doi.org/10.1016/j.ceramint.2011.05.002.

[26] B.H. Mo, H. Zhu, X.M. Cui, Y. He, S.Y. Gong, Effect of curing temperature on geopolymerization of metakaolin-based geopolymers, Appl. Clay Sci. (2014). https://doi.org/10.1016/j.clay.2014.06.024.

[27] M.S. Muñiz-Villarreal, A. Manzano-Ramírez, S. Sampieri-Bulbarela, J.R. Gasca-Tirado, J.L. Reyes-Araiza, J.C. Rubio-Ávalos, J.J. Pérez-Bueno, L.M. Apatiga, A. Zaldivar-Cadena, V. Amigó-Borrás, The effect of temperature on the geopolymerization process of a metakaolin-based geopolymer, Mater. Lett. (2011). https://doi.org/10.1016/j.matlet.2010.12.049.

[28] P. Rovnaník, Effect of curing temperature on the development of hard structure of metakaolin-based geopolymer, Constr. Build. Mater. (2010). https://doi.org/10.1016/j.conbuildmat.2009.12.023.

[29] R.C. Kaze, L.M. Beleuk à Moungam, M.L. Fonkwe Djouka, A. Nana, E. Kamseu, U.F. Chinje Melo, C. Leonelli, The corrosion of kaolinite by iron minerals and the effects on geopolymerization, Appl. Clay Sci. (2017). https://doi.org/10.1016/j.clay.2016.12.040.

[30] C.R. Kaze, H.K. Tchakoute, T.T. Mbakop, J.R. Mache, E. Kamseu, U.C. Melo, C. Leonelli, H. Rahier, Synthesis and properties of inorganic polymers (geopolymers) derived from Cameroon-meta-halloysite, Ceram. Int. (2018). https://doi.org/10.1016/j.ceramint.2018.07.070.

[31] E. Adesanya, K. Ohenoja, J. Yliniemi, M. Illikainen, Mechanical transformation of phyllite mineralogy toward its use as alkali-activated binder precursor, Miner. Eng. (2020). https://doi.org/10.1016/j.mineng.2019.106093.

[32] L.N. Tchadjié, J.N.Y. Djobo, N. Ranjbar, H.K. Tchakouté, B.B.D. Kenne, A. Elimbi, D. Njopwouo, Potential of using granite waste as raw material for geopolymer synthesis, Ceram. Int. (2016). https://doi.org/10.1016/j.ceramint.2015.10.091.

[33] O. Vogt, N. Ukrainczyk, C. Ballschmiede, E. Koenders, Reactivity and microstructure of metakaolin based geopolymers: Effect of fly Ash and liquid/solid contents, Materials (Basel). (2019). https://doi.org/10.3390/ma12213485.

[34] M. Esaifan, H. Rahier, A. Barhoum, H. Khoury, M. Hourani, J. Wastiels, Development of inorganic polymer by alkali-activation of untreated kaolinitic clay: Reaction stoichiometry, strength and dimensional stability, Constr. Build. Mater. (2015). https://doi.org/10.1016/j.conbuildmat.2015.04.034.

[35] P.N. Lemougna, U.F. Chinje Melo, M.P. Delplancke, H. Rahier, Influence of the activating solution composition on the stability and thermo-mechanical properties of inorganic polymers (geopolymers) from volcanic ash, Constr. Build. Mater. (2013). https://doi.org/10.1016/j.conbuildmat.2013.06.089.

[36] ASTM, Standard Test Method for Compressive Strength of Hydraulic Cement Mortars, ASTM Int. (2012). https://doi.org/10.1520/C0109.

[37] ASTM C 642-2006, Standard test method for density, absorption, and voids in hardened concrete, ASTM Int. West Conshohocken, PA. (2006) 1–3. https://doi.org/10.1520/C0642-13.5.

[38] ASTM C157, StandardTest Method for Length Change of Hardened Hydraulic-Cement Mortar and, Annu. B. ASTM Stand. (2016). https://doi.org/10.1520/C0157.

[39] K.C. Gomes, G.S.T. Lima, S.M. Torres, S. De Barros, I.F. Vasconcelos, N.P. Barbosa, Iron distribution in geopolymer with ferromagnetic rich precursor, in: Mater. Sci.

Forum, 2010. https://doi.org/10.4028/www.scientific.net/MSF.643.131.

[40] R.I. Iacobescu, V. Cappuyns, T. Geens, L. Kriskova, S. Onisei, P.T. Jones, Y. Pontikes, The influence of curing conditions on the mechanical properties and leaching of inorganic polymers made of fayalitic slag, Front. Chem. Sci. Eng. (2017). https://doi.org/10.1007/s11705-017-1622-6.

[41] A. Peys, L. Arnout, T. Hertel, R.I. Iacobescu, S. Onisei, L. Kriskova, H. Rahier, B. Blanpain, Y. Pontikes, THE USE OF ATR-FTIR SPECTROSCOPY IN THE ANALYSIS OF IRON-SILICATE INORGANIC POLYMERS, n.d. http://slag-valorisation-symposium.eu/2017/wp-content/uploads/downloads/Session 5/Arne Peys - Paper - The use of ATR-FTIR spectroscopy in the analysis of iron-silicate inorganic polymers - SVS2017.pdf (accessed May 29, 2020).

[42] A. Nana, J. Ngouné, R.C. Kaze, L. Boubakar, S.K. Tchounang, H.K. Tchakouté, E. Kamseu, C. Leonelli, Room-temperature alkaline activation of feldspathic solid solutions: Development of high strength geopolymers, Constr. Build. Mater. (2019). https://doi.org/10.1016/j.conbuildmat.2018.11.068.

[43] G. Lecomte-Nana, H. Goure-Doubi, A. Smith, A. Wattiaux, G. Lecomte, Effect of iron phase on the strengthening of lateritic-based “geomimetic” materials, Appl. Clay Sci. (2012). https://doi.org/10.1016/j.clay.2012.09.014.

[44] Y. Pontikes, L. Machiels, S. Onisei, L. Pandelaers, D. Geysen, P.T. Jones, B. Blanpain, Slags with a high Al and Fe content as precursors for inorganic polymers, Appl. Clay Sci. (2013). https://doi.org/10.1016/j.clay.2012.09.020.

[45] S. Onisei, A.P. Douvalis, A. Malfliet, A. Peys, Y. Pontikes, Inorganic polymers made of fayalite slag: On the microstructure and behavior of Fe, J. Am. Ceram. Soc. (2018). https://doi.org/10.1111/jace.15420.

[46] D.L. Gallup, Iron silicate scale formation and inhibition at the salton sea geothermal field, Geothermics. (1989). https://doi.org/10.1016/0375-6505(89)90015-1.

[47] F. Puertas, T. Amat, A. Fernández-Jiménez, T. Vázquez, Mechanical and durable behaviour of alkaline cement mortars reinforced with polypropylene fibres, Cem. Concr. Res. (2003). https://doi.org/10.1016/S0008-8846(03)00222-9.

[48] M. Esaifan, H. Khoury, I. Aldabsheh, H. Rahier, M. Hourani, J. Wastiels, Hydrated lime/potassium carbonate as alkaline activating mixture to produce kaolinitic clay based inorganic polymer, Appl. Clay Sci. (2016). https://doi.org/10.1016/j.clay.2016.03.026.

[49] J.N. Yankwa Djobo, A. Elimbi, H. Kouamo Tchakouté, S. Kumar, Mechanical properties and durability of volcanic ash based geopolymer mortars, Constr. Build. Mater. (2016). https://doi.org/10.1016/j.conbuildmat.2016.07.141.

[50] C. Ridtirud, P. Chindaprasirt, K. Pimraksa, Factors affecting the shrinkage of fly ash geopolymers, Int. J. Miner. Metall. Mater. (2011). https://doi.org/10.1007/s12613-011-0407-z.

[51] G. Görhan, R. Aslaner, O. Şinik, The effect of curing on the properties of metakaolin and fly ash-based geopolymer paste, Compos. Part B Eng. (2016). https://doi.org/10.1016/j.compositesb.2016.05.019.

[52] R.Y. Nkwaju, J.N.Y. Djobo, J.N.F. Nouping, P.W.M. Huisken, J.G.N. Deutou, L. Courard, Iron-rich laterite-bagasse fibers based geopolymer composite: Mechanical, durability and insulating properties, Appl. Clay Sci. (2019). https://doi.org/10.1016/j.clay.2019.105333.

[53] W.D.A. Rickard, L. Vickers, A. van Riessen, Performance of fibre reinforced, low

density metakaolin geopolymers under simulated fire conditions, Appl. Clay Sci. (2013). https://doi.org/10.1016/j.clay.2012.10.006.

[54] E. Kamseu, B. Ceron, H. Tobias, E. Leonelli, M.C. Bignozzi, A. Muscio, A. Libbra, Insulating behavior of metakaolin-based geopolymer materials assess with heat flux meter and laser flash techniques, in: J. Therm. Anal. Calorim., 2012. https://doi.org/10.1007/s10973-011-1798-9.

[55] R.M. Novais, L.H. Buruberri, G. Ascensão, M.P. Seabra, J.A. Labrincha, Porous biomass fly ash-based geopolymers with tailored thermal conductivity, J. Clean. Prod. (2016). https://doi.org/10.1016/j.jclepro.2016.01.083.

[56] H. Assaedi, T. Alomayri, C.R. Kaze, B.B. Jindal, S. Subaer, F. Shaikh, S. Alraddadi, Characterization and properties of geopolymer nanocomposites with different contents of nano-CaCO3, Constr. Build. Mater. (2020). https://doi.org/10.1016/j.conbuildmat.2020.119137.

[57] J.N.Y. Djobo, D. Stephan, A. Elimbi, Setting and hardening behavior of volcanic ash phosphate cement, J. Build. Eng. (2020). https://doi.org/10.1016/j.jobe.2020.101427.